SAND2016-11315PE

Exceptional service in the national interest

Sandia National Laboratories

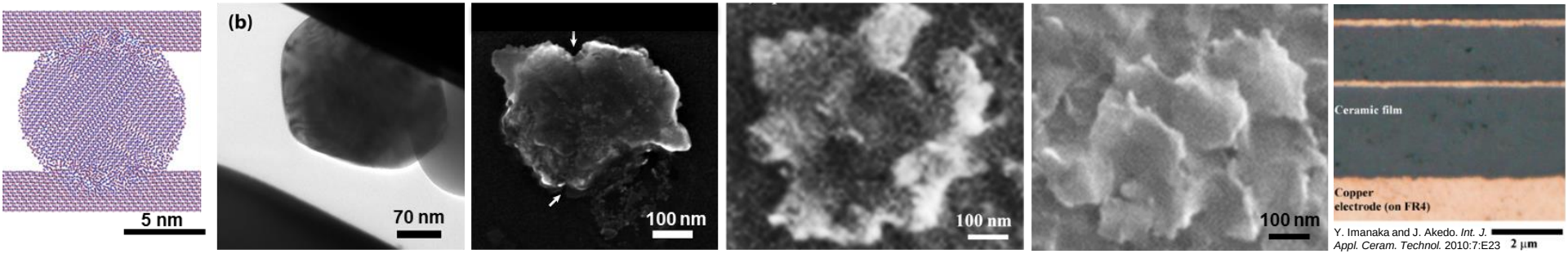

Fundamental Mechanisms Behind Room Temperature Aerosol Deposition for Fabrication of Meso-Scale Metallic & Ceramic Films

Pylin Sarobol, Andrew Vackel, Jesse Adamzcyk, and Thomas Holmes

National Labs @ Purdue Days, Nov 7-8, 2016

U.S. DEPARTMENT OF ENERGY | NNSA National Nuclear Security Administration

Sandia National Laboratories is a multi-mission laboratory managed and operated by Sandia Corporation, a wholly owned subsidiary of Lockheed Martin Corporation, for the U.S. Department of Energy's National Nuclear Security Administration under contract DE-AC04-94AL85000. SAND2015-3704C

Sandia National Laboratories, Materials Science Center

THERMAL SPRAY RESEARCH LAB - DEPARTMENT OF COATINGS & ADDITIVE MANUFACTURING

Thermal Spray Research Lab – TSRL

- Coatings and Additive Manufacturing Department, Materials Science Center


D. Hirschfeld


A. Hall


P. Sarobol


A. Vackel


A. Miller


A. Mayer


J. Padilla

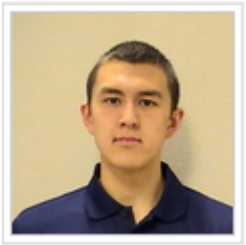
J. Adamczyk


T. Holmes


C. Silva


D. Beatty

Thermal Spray Technology

- Thermal spraying = coating processes in which heated/melted materials are deposited onto a surface.
- High deposition rate over large area. *mostly constrained by line-of-sight.
- Thickness range ~ 20 um to several mms, depending on process/feedstock.
- Quality assessed by measuring porosity, oxide content (in metallic coatings), hardness, bond strength and surface roughness. Generally, the coating quality increases with increasing particle velocities.

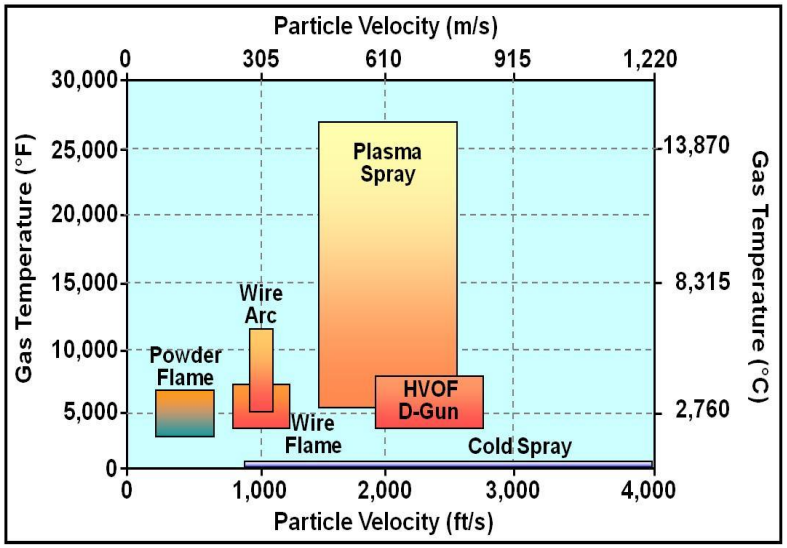

*Adapted from plots by R.C. McCune, Ford Motor Co. & A. Papyrin, Ktech Corp.

Different Thermal Spray processes allow access to different regimes of particle temperature and velocity space.

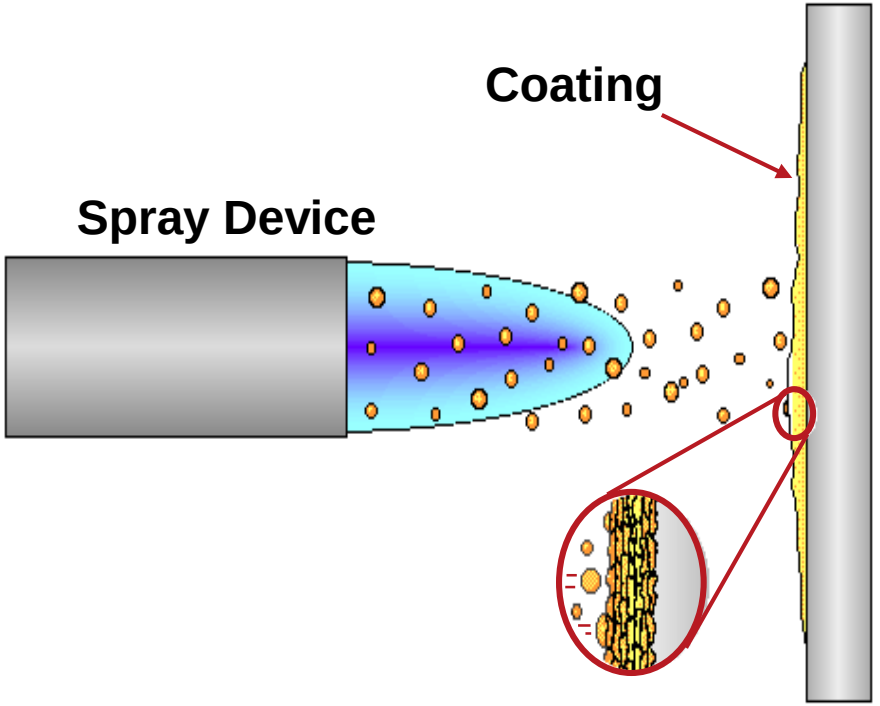

Particle Temperature & Velocity at impact determine coating microstructure and properties.

Sandia National Laboratories

SNL's Thermal Spray Research Lab

Sandia's TSRL is a broadly capable development facility with experience operating at least one version of every major thermal spray processes.

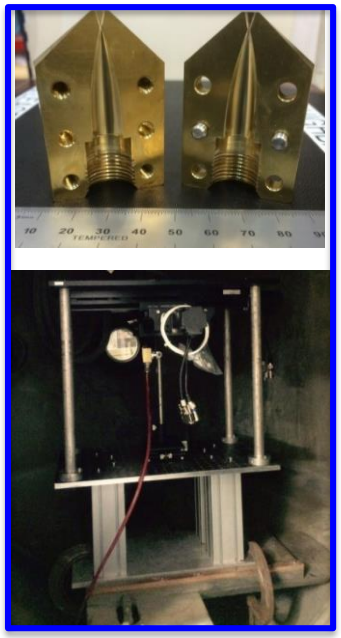

Aerosol Deposition

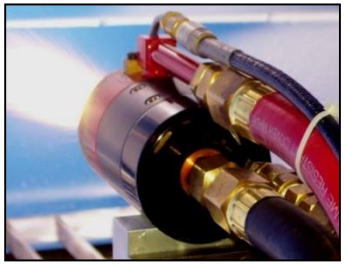

Atmospheric Plasma Spray

Twin Wire Arc Spray

Vacuum, low pressure, and very low pressure plasma spray

Cold Spray

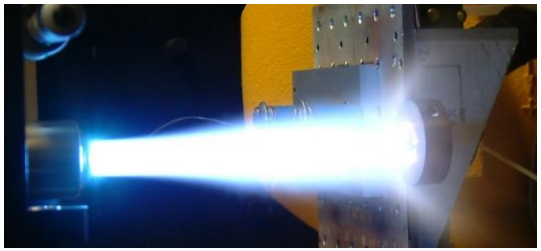

Powder Flame Spray

Wire Flame Spray

HVOF

Industrial Applications – Passive Coatings

- Aerospace
  - Gas Turbines
  - Landing Gear
- Automotive
- Biomedical
- Computers
- Infrastructure
- Marine
- Paper Making
- Petrochemical
- Power Generation
- Printing
- Textiles
- Electronics

Hydroxyapatite coating on a hip implant

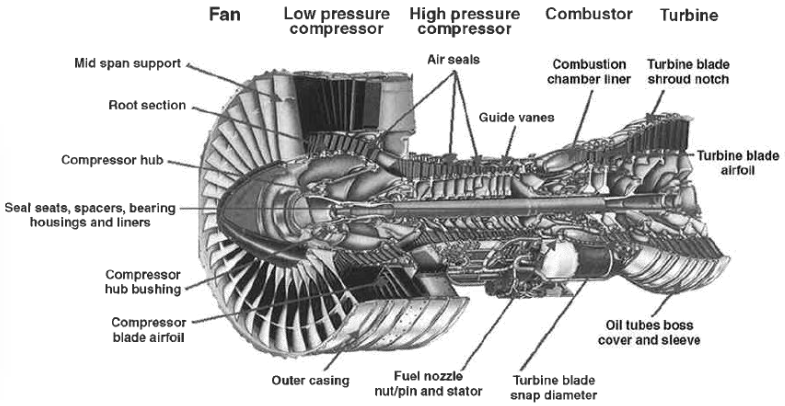

Gas Turbines are full of sprayed coatings!

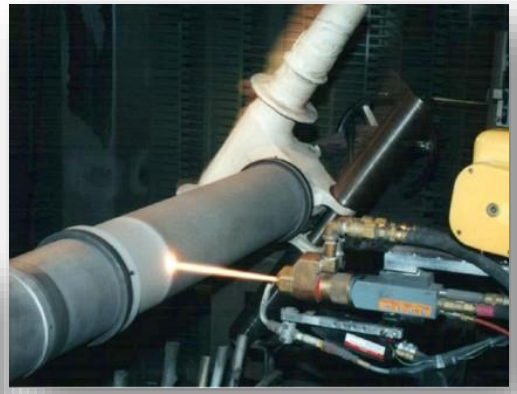

Hard Chrome Replacement on a Landing Gear Strut

The Wuhan Junshan Bridge over the Yangtze River is covered with 35,000 m^2 (~8.5 acres) of thermal sprayed zinc coating!

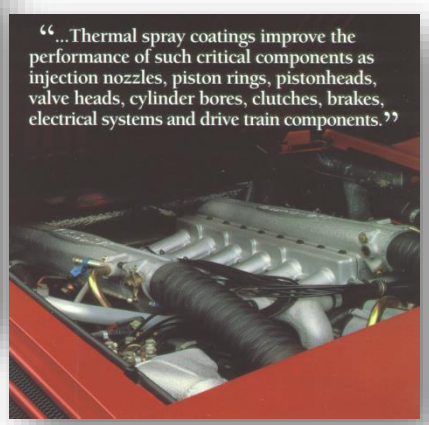

Auto applications include pistons, valves, cylinder bores, clutches, and drive train components.

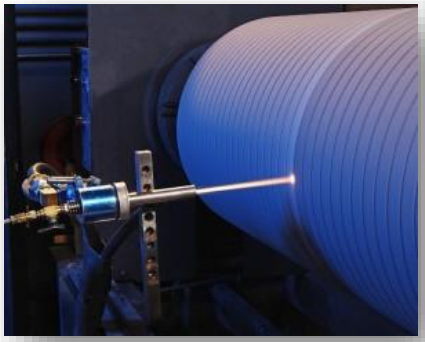

Ceramic Coating a Printing Roll

Thermal Spray Coatings find niche surface engineering/modification applications in many industries.

Current R&D Work – Active Coatings

Towards active/functional coatings, bridging the 10-µm–to–mm scale in fabricating mesoscale electronic devices and sensor materials

Asia
- Electronic Devices

Stony Brook University & Partners
- Multilayer inductor circuits
- Thermocouples
- Antennas
- Humidity sensors
- Magnetoresistive sensors

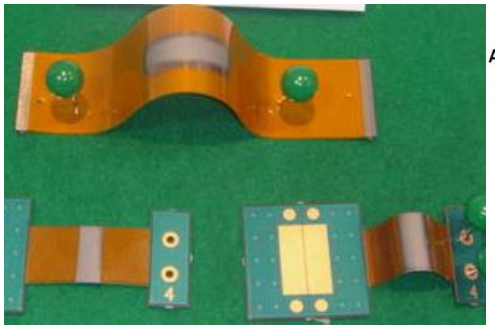

AD Flexible electronics from J. Akedo. *JTST.,* 2007:17:181

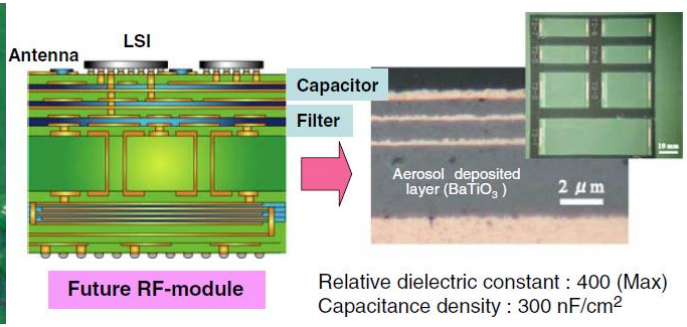

Y. Imanaka and J. Akedo, Integrated RF Module, Proceedings of the 54th ECTC 2004, p 1614-1620

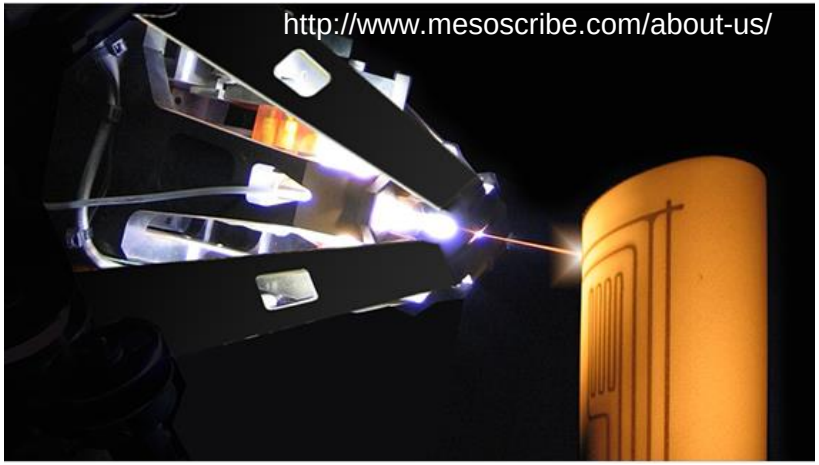

MesoScribe Technologies - Antennas, heaters, sensors, and wiring are integrated with structures or stand alone heaters, heat flux sensors, and crack detection sensors.

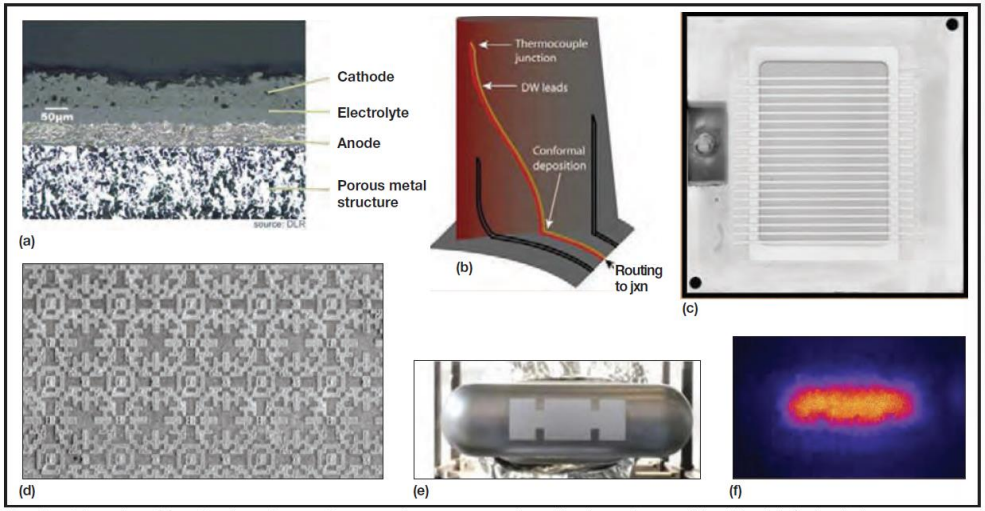

Fig. 1 — *Examples of functional coatings and patterned structures produced by thermal spray: (a) solid oxide fuel cells (courtesy Juelich Research Center), (b) direct write antenna, (c) illustration of direct write, thermal sprayed thermocouple on component (courtesy Mesoscribe Tech.), (d) actual instrumented components built, (e) multilayer inductor fabricated with blanket and direct write thermal spray, and (f) proton scintillator coatings as made and with protons.*

Sampath et al. iTSSe ADVANCED MATERIALS & PROCESSES • NOVEMBER-DECEMBER 2013

LDRD

Laboratory Directed Research and Development

Sandia National Laboratories

- Michael Chandross
- William M. Mook
- Paul G. Kotula
- Daniel C. Bufford
- Khalid Hattar,
- Brad L. Boyce
- Jay D. Carroll
- Andrew Vackel
- Jesse Adamczyk
- Thomas D. Holmes
- Andrew S. Miller
- Aaron C. Hall
- David E. Beatty
- Andrew J. Mayer
- Deidre Hirschfeld
- Harlan Brown-Shaklee
- Adam W. Cook
- Donald F. Susan
- Rick A. Kellogg
- Bonnie B. McKenzie
- David M. Keicher

A (nominal) room temperature process to deposit ceramic coatings

AEROSOL DEPOSITION

Deposition Processes

Aerosol Deposition bridges the gap between traditional thin film and thermal spray thick film technologies. It also enables materials integration at room temperature.

Process Parameters	PVD ("Thin" Films)	Aerosol Deposition	Thermal Spray ("Thick" Films)
Temperature	>500 °C	20 °C	>1000 °C
Max Film thickness	5 µm	100 µm	1 mm
Grain Size	10-100 nm	10-100 nm	10-100 µm
Typical Microstructures	Dense, Columnar	Dense, Nanocrystalline	Some Porosity, Lamellar

Microstructures of PVD, AD, and TS coatings

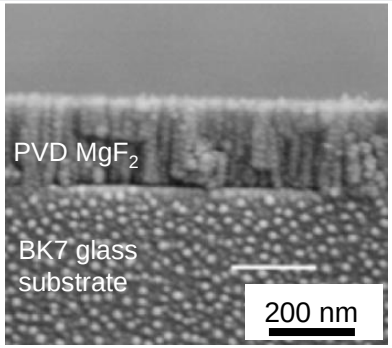

Physical Vapor deposited columnar MgF_2

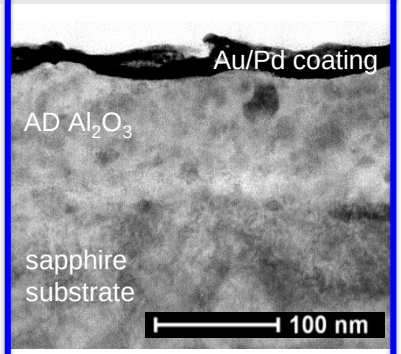

Aerosol deposited Al_2O_3 on Sapphire substrate

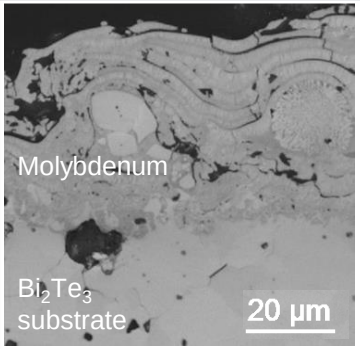

Plasma sprayed Mo On Bi_2Te_3 Substrate

C. Guo, et al., *Opt. Express*, vol. 21, no. 1, pp. 960-967, 2013.

Solid-State Deposition of Ceramics

Ceramics are conventionally processed at >700°C. A room temperature (RT), solid-state deposition process eliminates high processing temperature, enabling materials integration.

Aerosol Deposition (AD)

- Only several systems and researchers in the world.
  J. Akedo, Y. Imanaka, D.-S. Park, C. Lee, D.M. Chun, R. Moos, S. Johnson (NRL), P. Fuierer (NMIMT), etc.
- AD process at RT in vacuum
  - sub-micron particles accelerated to high velocity by pressurized gas, impacted, consolidated to form films.
-

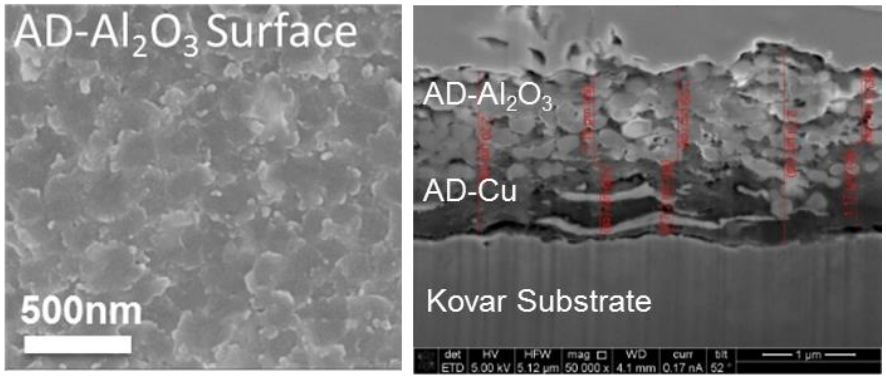

SNL AD graded Cu-Al_2O_3 film

Aerosol Deposition is significant because it allows materials integration.
- Process = 20°C.
- Al_2O_3 T_m = 2100°C.
- Kovar T_m = 1450°C.
- Cu T_m = 1085°C.

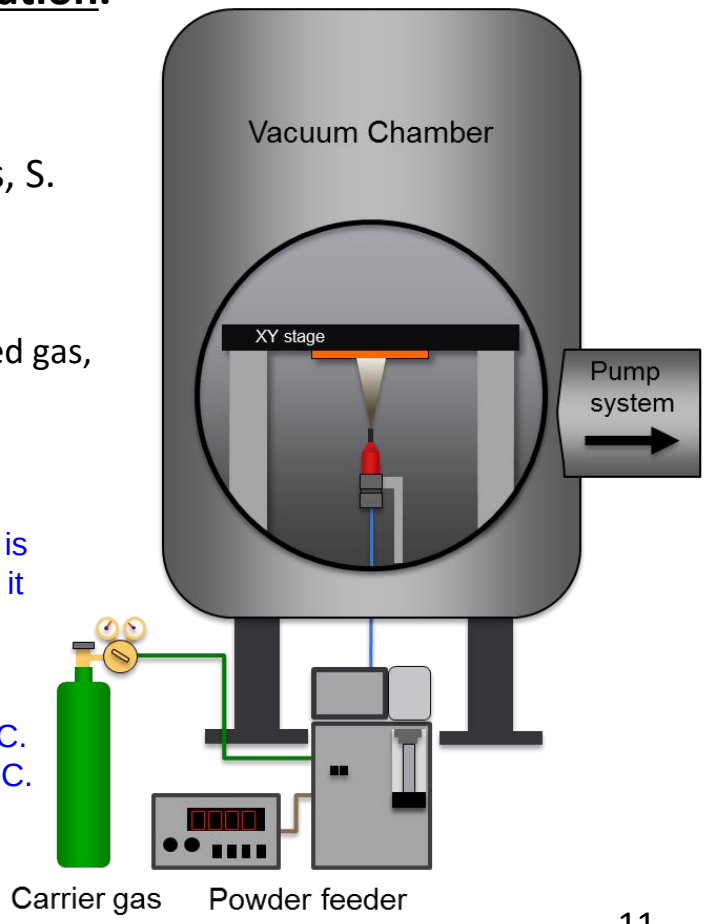

Solid-State Deposition of Ceramics

Ceramics are conventionally processed at >700°C. A room temperature (RT), solid-state deposition process eliminates high processing temperature, enabling materials integration.

Aerosol Deposition (AD)

- Only several systems and researchers in the world.
  J. Akedo, Y. Imanaka, D.-S. Park, C. Lee, D.M. Chun, R. Moos, S. Johnson (NRL), P. Fuierer (NMIMT), etc.
- AD process at RT in vacuum
  - sub-micron particles accelerated to high velocity by pressurized gas, impacted, consolidated to form films.
- Similar AD ceramic film microstructures
  - sub-micron particles undergo *plastic deformation*
  - break up into *small crystallites* (20-75 nm) [1-3]
  - planar *defects* and *amorphous regions* [4].
- Need to understand fundamental mechanisms behind ceramic particle deformation and bonding.

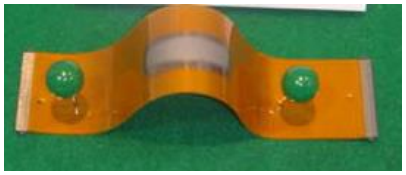

AD Flexible electronics from J. Akedo. *JTST.*, 2007:17:181

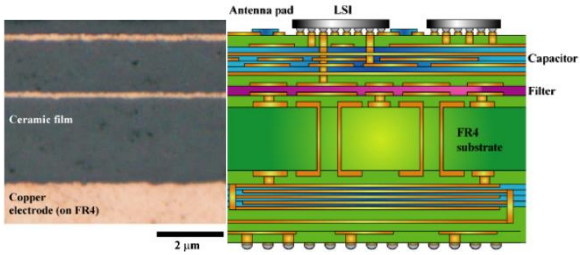

AD multi-layer capacitor from Y. Imanaka and J. Akedo. *Int. J. Appl. Ceram. Technol.* 2010:7:E23

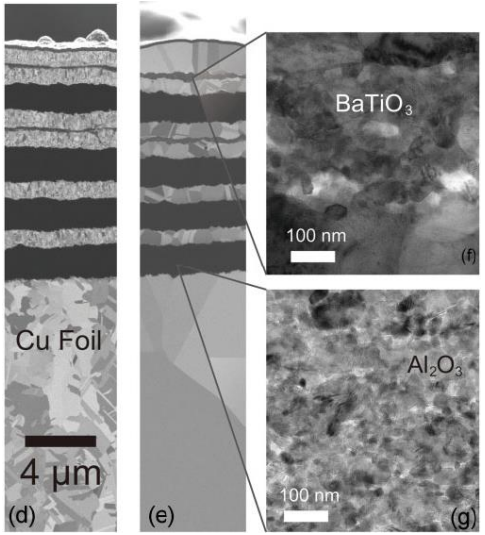

$BaTiO_3/Al_2O_3$/Cu multi-layered structure produced by AD and electroplating from Y. Imanaka *et al. Adv Engr Mater.*, 2013:15:1129

[1] Akedo, J. and Ogiso, H., *JTST*, Vol. 17, (2008), pp. 181-198.
[2] Akedo, J., *JTST*, Vol. 17, (2008), pp. 181-198.
[3] Akedo, J. *J. Am. Ceram. Soc.*, Vol. 89, (2006), pp. 1834-1839.
[4] Park, H. *et al*. Scripta Materialia, 2015.

Project Technical Highlights

- New film deposition capability
- Understand sub-micron ceramic particles RT deformation as a building block for AD coatings.
  - Simulations and experiments were in agreement.
    - Quasi-static loading – particle compressions
    - High strain-rate loading – impacts on deposition
- Used the knowledge gained and demonstrated aerosol deposited ceramic, metallic, and composite coatings and integration.

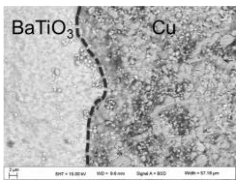

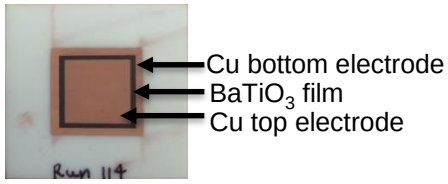

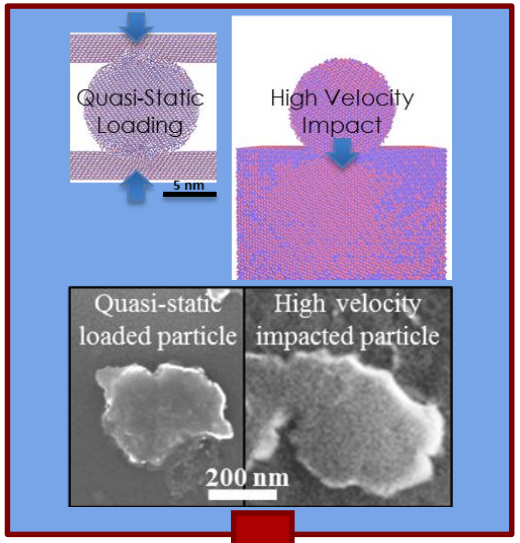

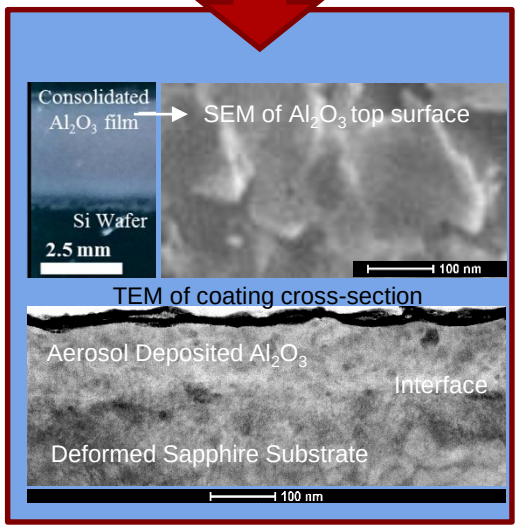

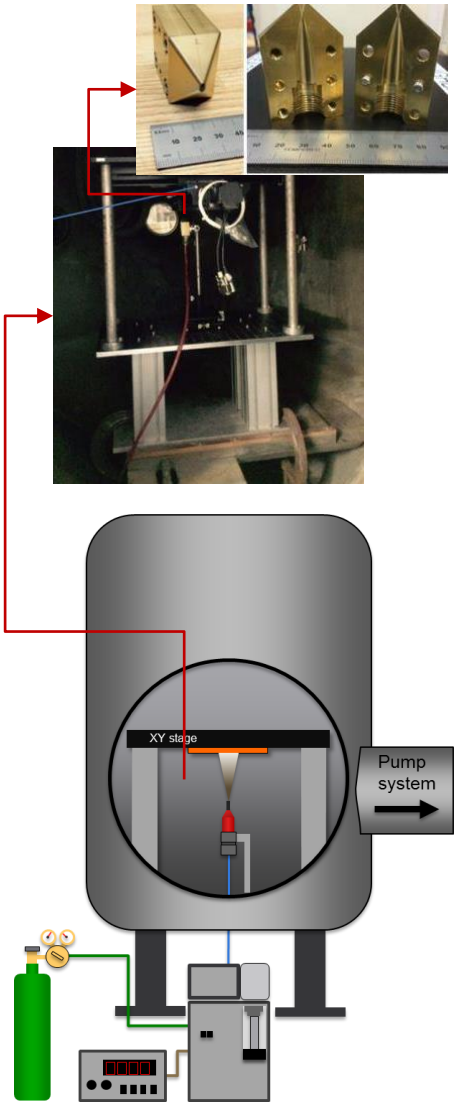

Sandia National Laboratories

COMPRESSION STUDY

Quasi-static Loading - Particle compression simulation and experiments.

DEPOSITION STUDY

High Strain-Rate Loading – Single particle impact and coating experiments.

IDENTIFYING DEFORMATION AND CONSOLIDATION MECHANISM

Materials Response to Loading

- Ductile vs. Brittle
- Bulk materials with high degrees of covalent/ionic bonding, e.g. ceramics, typically undergo **BRITTLE** fracture when strained.
  - a combination of limited fracture toughness and preexisting flaws.
  - The role of pre-existing flaws and defects can evolve as the characteristic length scale of materials decrease (e.g. micro-pillars and particles) [1-14]. In bulk ceramics →crack initiation sites.

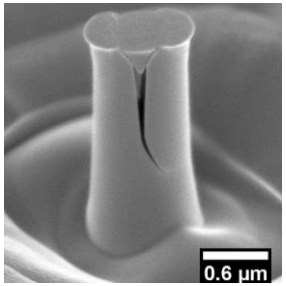

http://phys.org/news/2009-10-silicon-brittle-kind.html

http://web.mit.edu/dlizardo/www/UniaxialTestingLabReportV6.pdf

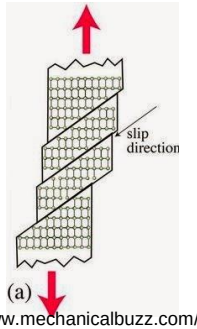

http://www.mechanicalbuzz.com/2014/10/plastic-deformation-slip-and-twinning.html

Brittle – Crack nucleation and propagation

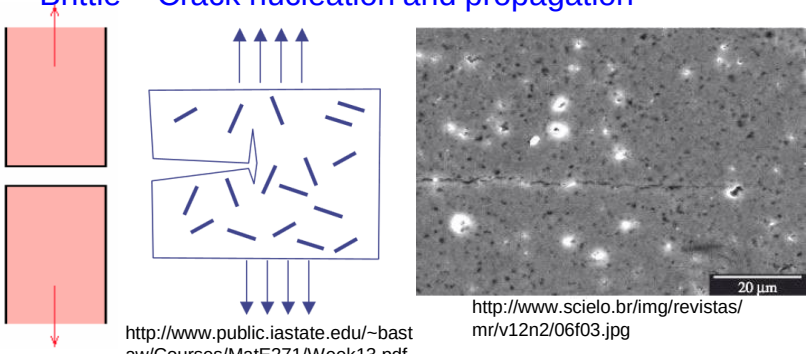

http://www.public.iastate.edu/~bastaw/Courses/MatE271/Week13.pdf

http://www.scielo.br/img/revistas/mr/v12n2/06f03.jpg

VS.

Ductile – **Dislocation Mediated/Plasticity → Shape Change**

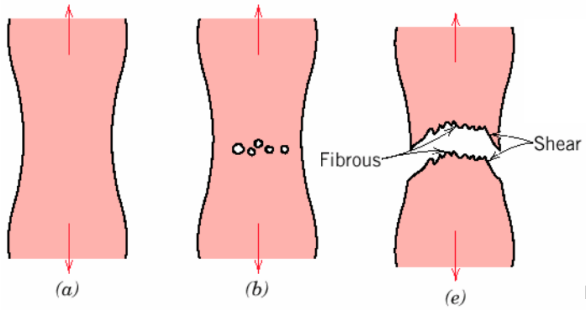

http://people.virginia.edu/~lz2n/mse209/Chapter8.pdf

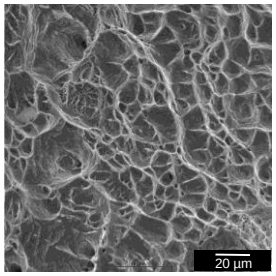

http://gradel.lu/activites/nitruration-traitement-thermique/analyse-metallurgique/

Materials Response to Loading

- Ductile vs. Brittle
- **At small length scales, significant plasticity (deformation) observed in ceramic single crystals at room temperatures.**
  - Low strain rates → compressed micro-pillars & particles
  - High strain rates → aerosol deposition (AD)
- Room temperature plasticity in ceramics at small length scale gave insights into future development of *alternative ceramic forming technology* and high strength/high toughness functional ceramics.

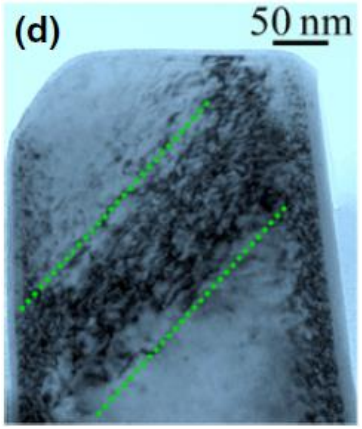

Dislocations on {001} planes in compressed ZrC pillar from S. Kiani, *et al.* *J. Am. Ceram. Soc.*, 2015:98:2313

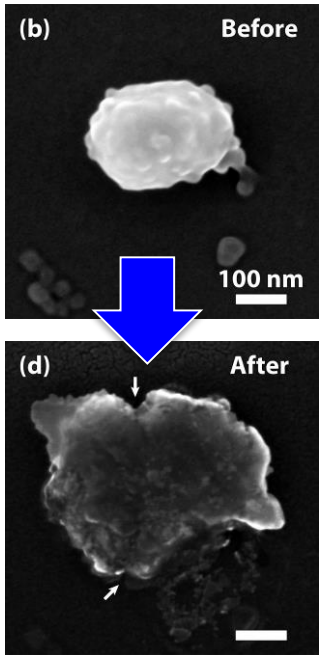

P. Sarobol, *et al.*, *JTST.*, 2016:25

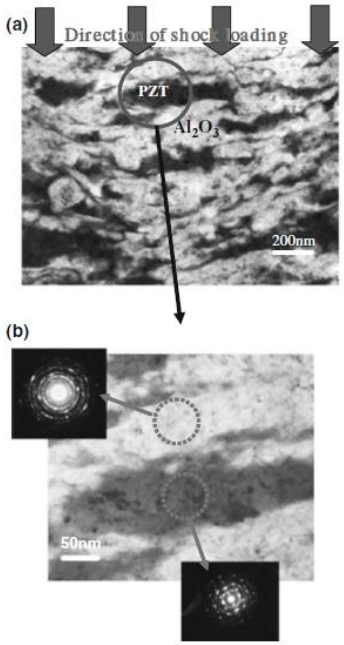

J. Akedo. *JTTEE5.*, 2007:17:181

Dislocation Plasticity (shape change) and Fracture

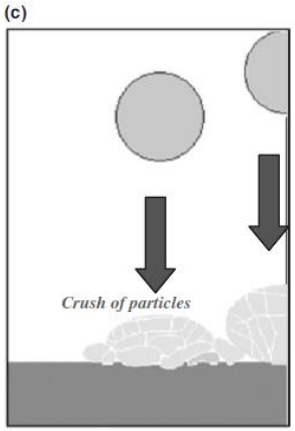

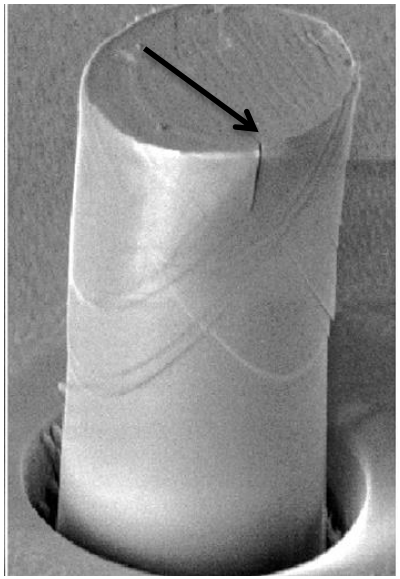

Compressed AlN pillar showing plastic deformation and cracking. J.J. Guo et al. / Acta Materialia 88 (2015) 252–259

Particle Compression Study

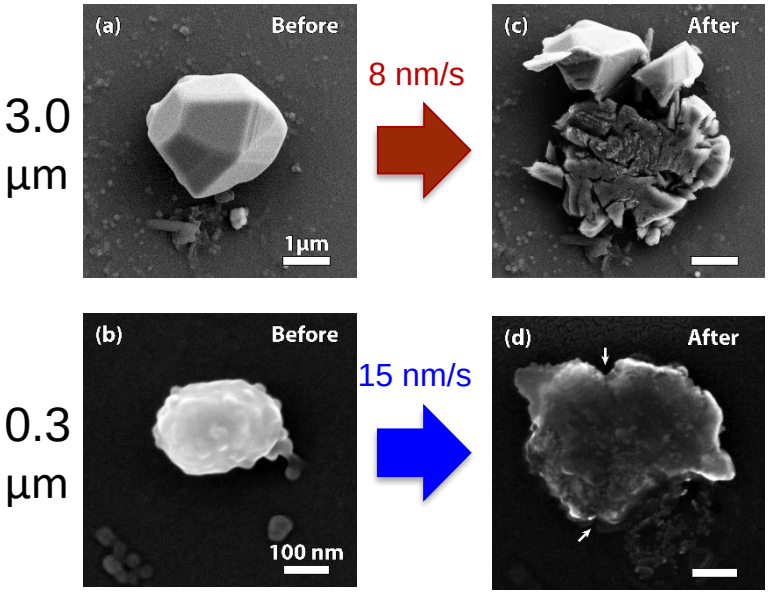

Particle Identifier	Diameter (µm)	Nominal Strain Rate (s^{-1})	Strain Energy before Fracture (MJ/m^3)	Strain at Fracture (%)
Large Particles				
SEM-LP1	2.9	0.03	47	5
SEM-LP2	2.6	0.006	106	5
SEM-LP4	2.9	0.005	70	5
SEM-LP5	2.9	0.003	203	7
Avg Large Particles	**2.8**	-	**106±69**	**5.5 ± 1**
Small Particles				
SEM-SP2	0.17	0.09	494	11
SEM-SP3	0.29	0.05	366	12
SEM-SP4	0.28	0.05	607	13
SEM-SP5	0.29	0.05	675	16
*TEM-SA2	0.38	*0.005	573	32
*TEM-SB1	0.24	*0.009	1066	27
Avg Small Particles	**0.26**	-	**630±238**	**18 ± 9**

Use submicron sized particles for feedstock

- Micron sized particles - brittle fracture
- Sub-micron sized particles - substantial plastic deformation before fracture.
  - 6x higher strain energy density input
    - dislocation nucleation
  - 3x higher accumulated strain
- In some cases, became polycrystalline.
- Takes more energy to nucleate dislocations and move them for deformation.

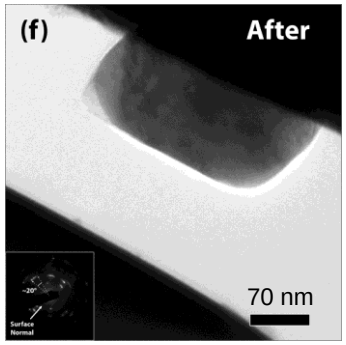

***In Situ* TEM compression of 0.3µm particle – dislocation plasticity, fracture, polycrystallinity**

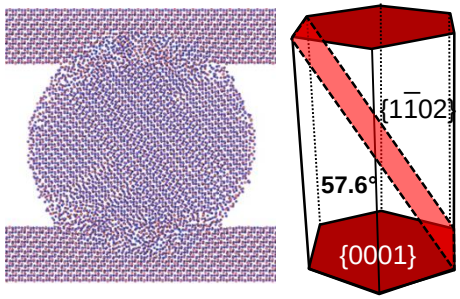

MD simulation of 10 nm particle – dislocations on Rhombohedral planes

In Situ TEM Compression

Sandia National Laboratories

In Situ Micro-Compression[5] – 300 nm particles

- Single crystal, ultra pure 300 nm sapphire (α-Al_2O_3) particles.
- A Hysitron PI95 TEM Picoindenter with a 1 µm diameter flat punch tip and the a JEOL 2100 LaB_6 TEM[7] at 200 kV were used.
- Compression done in ***open loop*** mode with the loading rate of 10 µN/s (approx. **< 2 nm/s** displ rate). Images taken at 15 fps.

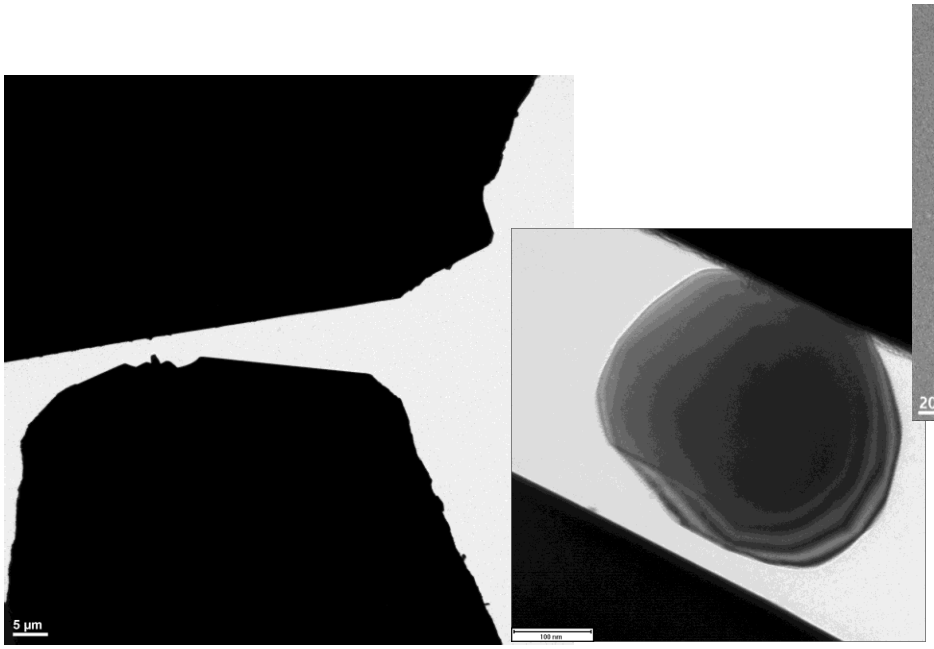

***In situ* TEM micro-compression on 0.3µm particle**

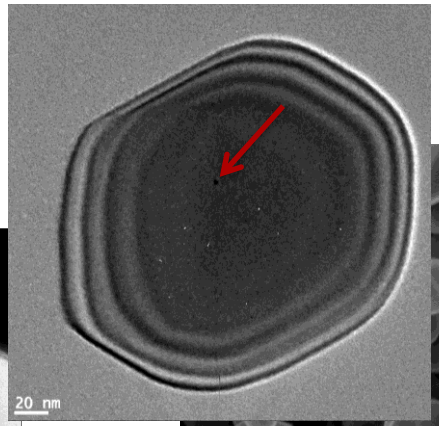

Bright field TEM image of a 300 nm particle oriented on the [001] zone axis.

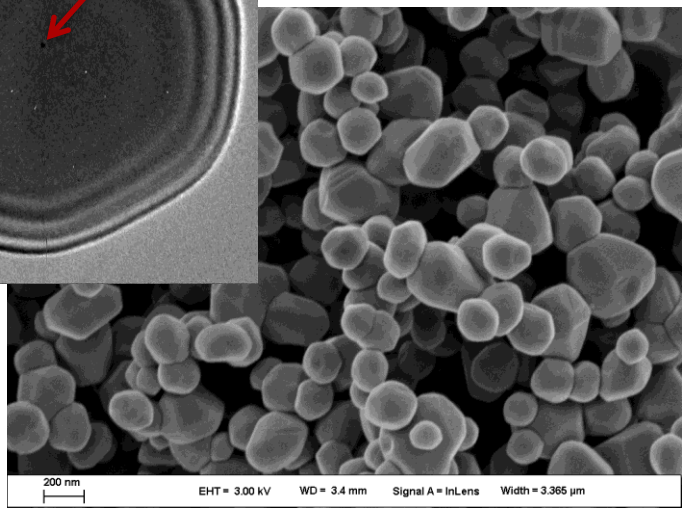

SE SEM image of the 300 nm

[5] Sarobol, P., *et al*., *SAND2014-18127*, (2014).
[6] Hysitron I (2013) SEM Picoindenter User Manual. Revision 9.3.0913 edn.
[7] Hattar, K., et al., Nuclear Instruments and Methods in Physics Research B. Vol. 338, (2014), pp. 56–65.

In Situ TEM Compression

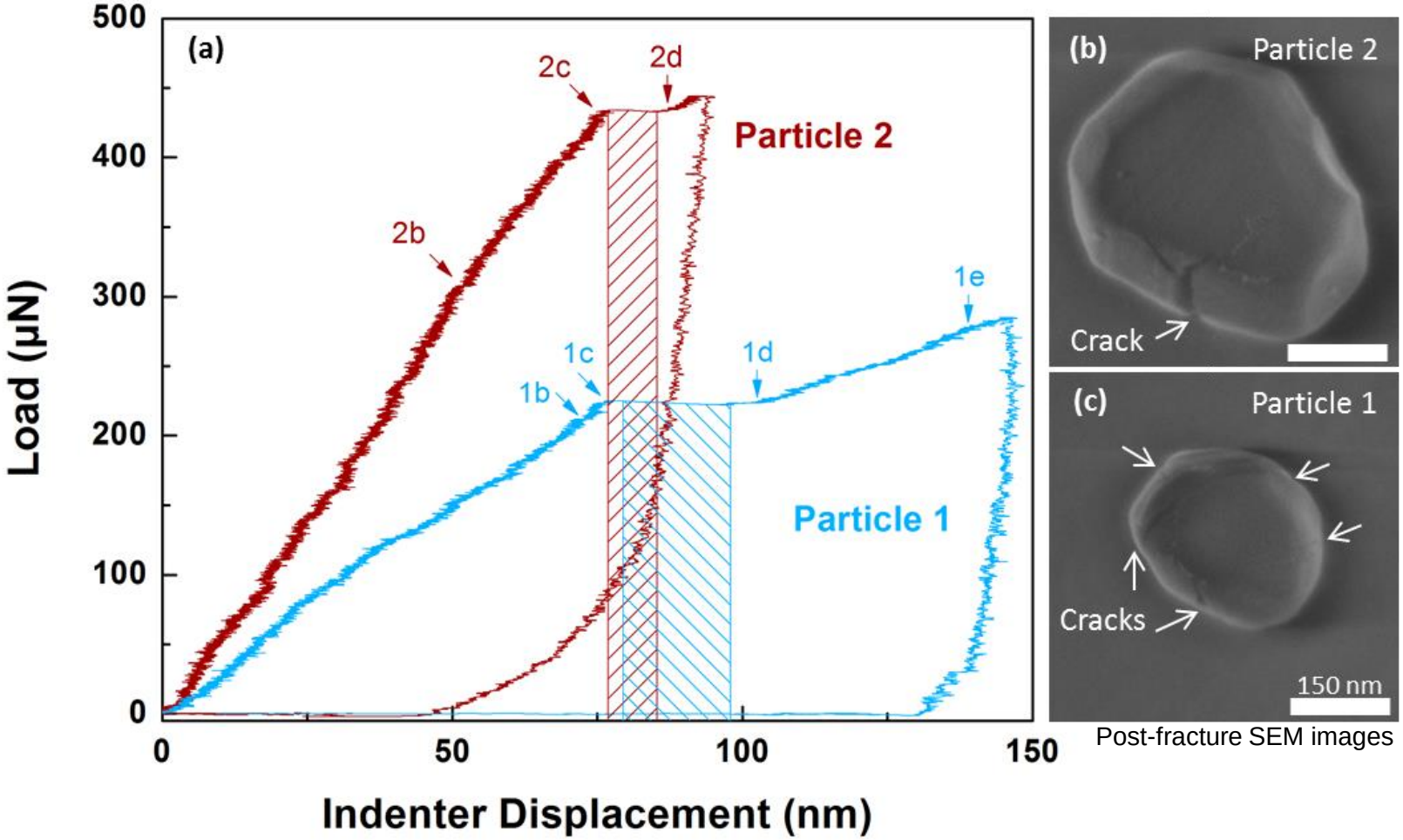

Post-fracture SEM images

- Elastic to Plastic transitions are unclear. Seemed to happen much earlier in the loading (first 5-10 nm displacement). Absence of concavity and linearity of the curves were surprising.
- G_C values for Particle 1 and 2 are 45 J/m^2 and 17 J/m^2, respectively. Values within the calculated range of orientation-dependent G_C of single crystal alumina of 16 - 65 J/m^2 [47].

In Situ TEM Compression – P1

Sandia National Laboratories

Zone axis near $[\bar{9}\,\bar{9}\,18\,6]$

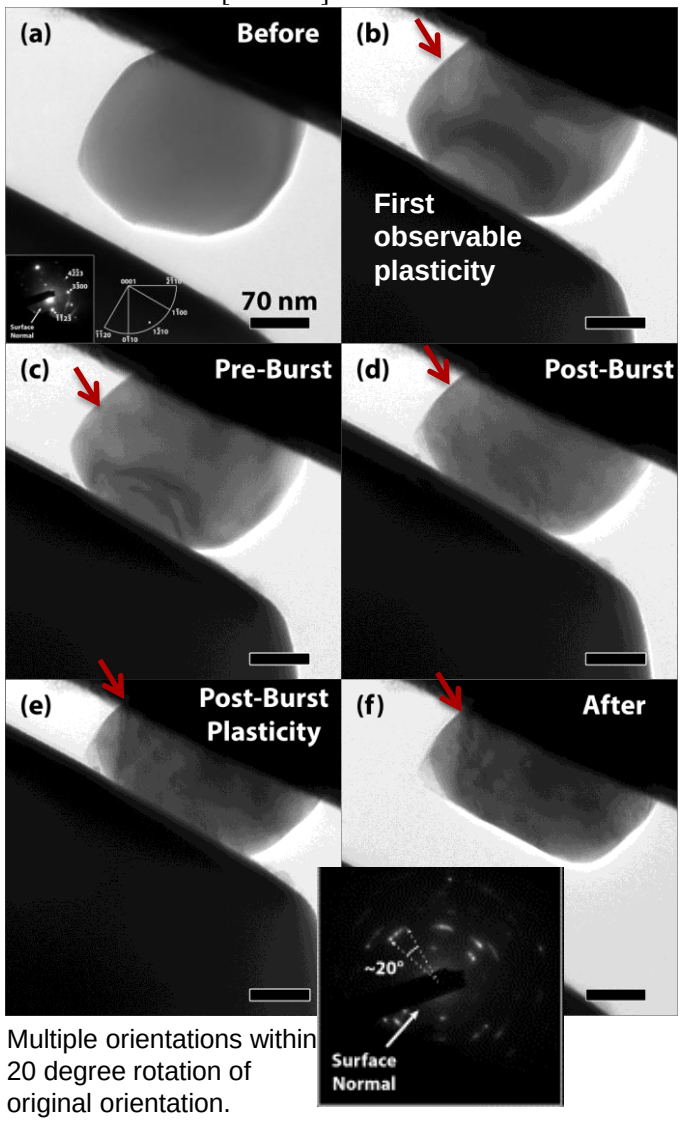

Multiple orientations within 20 degree rotation of original orientation.

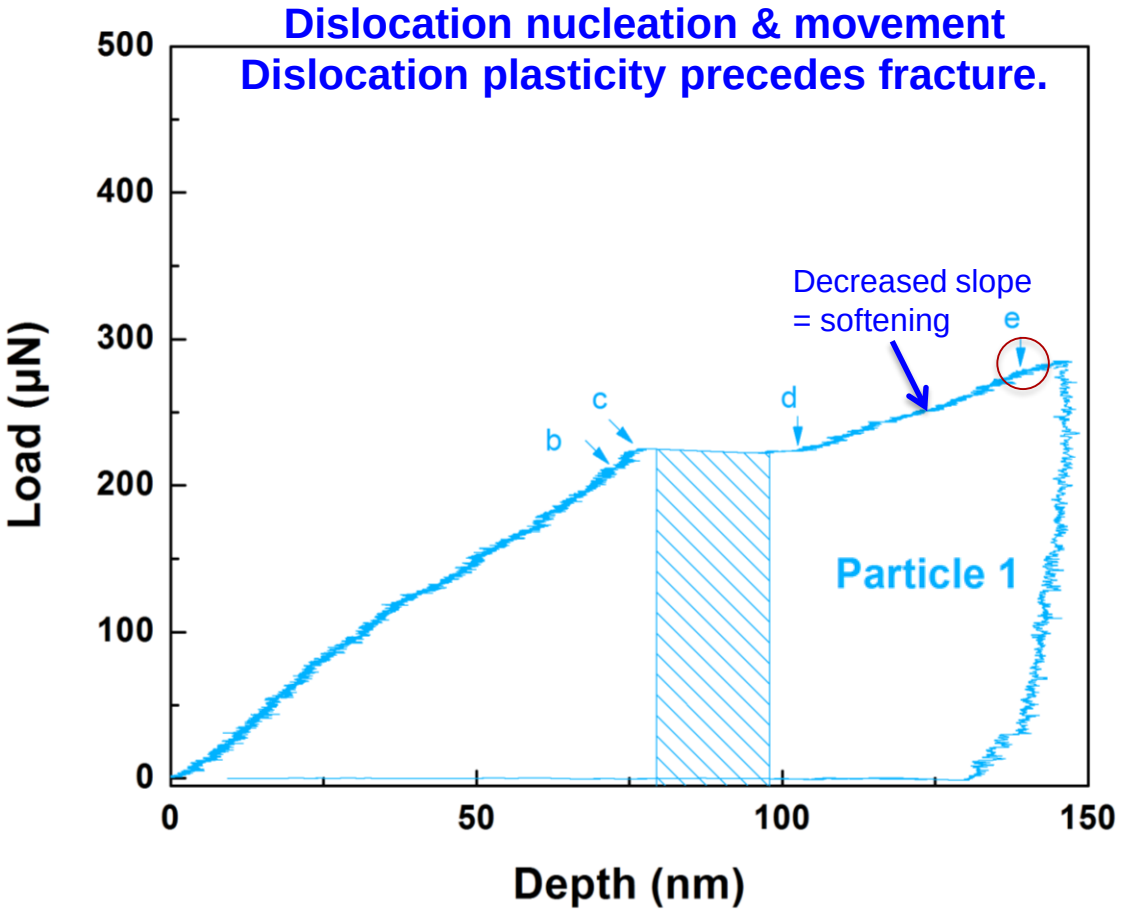

- Pre-burst plasticity: small regime with low dislocation activity.
- **Crack nucleation and propagation** leading to through-particle fracture.
- Post-burst plasticity: high dislocation activities, change in deformation mechanism as indicated by lower slope.
- **Mosaicity** with a 20 degree orientation spread.

In Situ TEM Compression – P1

Diameter ~ 0.24 μm, Open loop, Strain rate ~ 0.009 s^{-1}

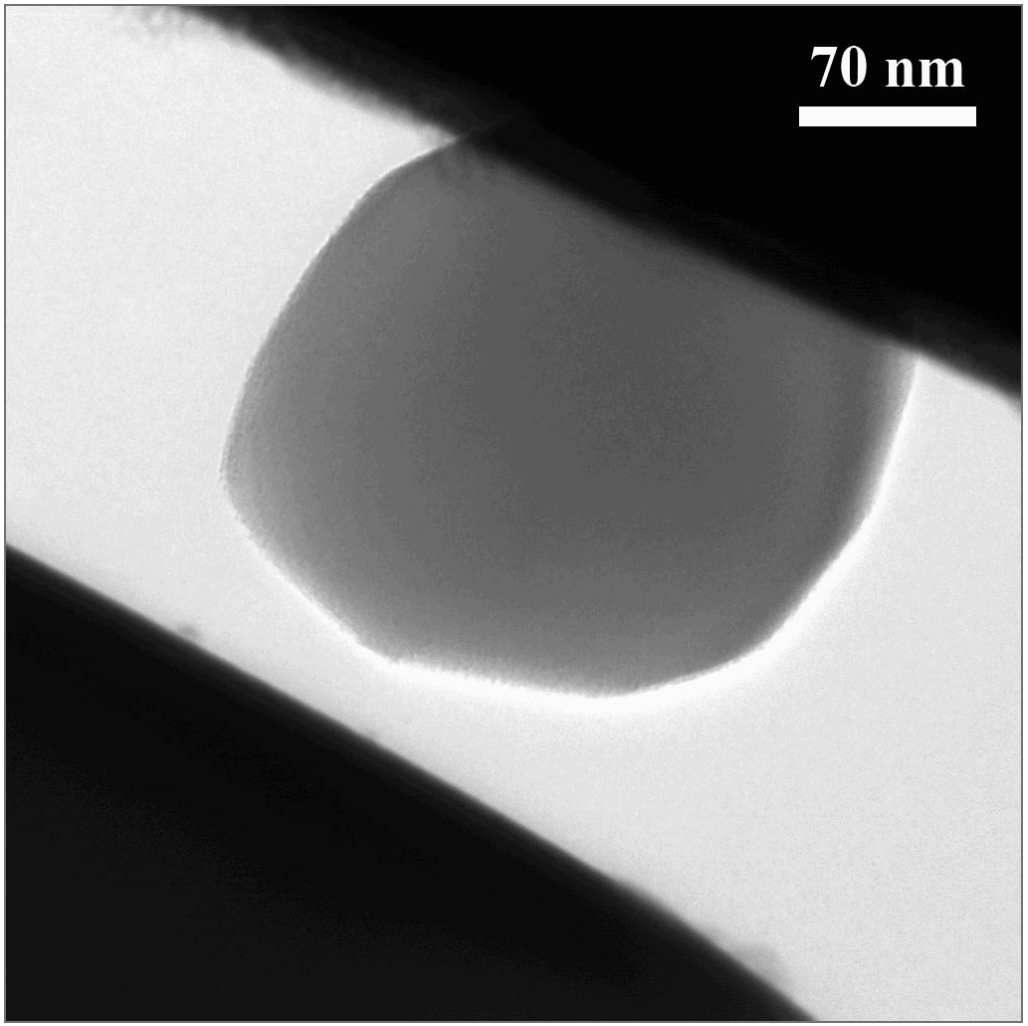

Dislocation nucleation & movement
Dislocation plasticity precedes fracture.

Large displacement gain at a constant load ("burst") corresponds to particle fracture.

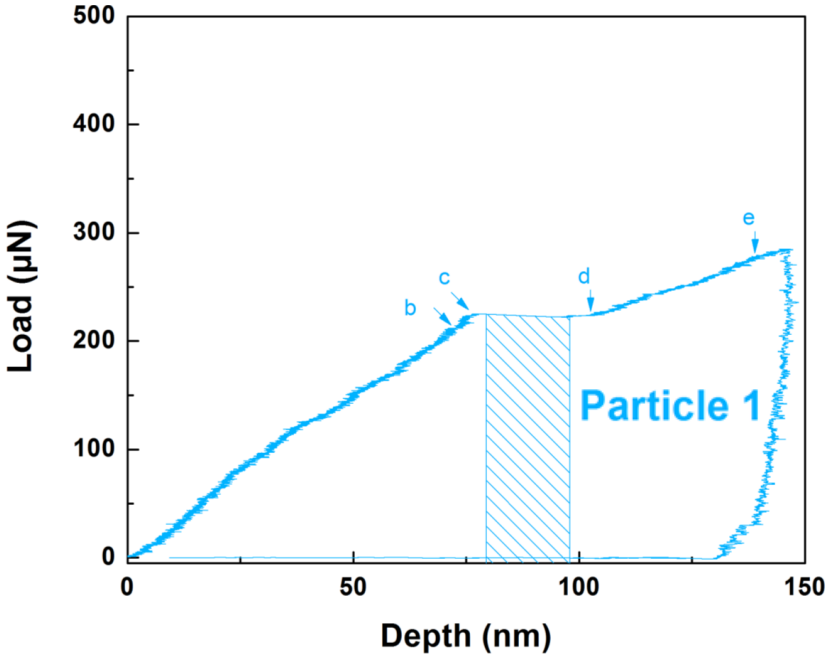

Simulated Particle Compression

Molecular Dynamics Simulations – 10 nm nanoparticles (NPs)

- MD allows identification of dislocations, slip planes, and particle fracture.
- Long computing time to simulate size > 50 nm (~36 million atoms)
- Simulating 10 nm sapphire nanoparticle (NP) (~300,000 atoms)
- A force-field for ceramics, developed by Garofalini[8].
- NPs were compressed (by ~1/3 of the initial diameter) between sapphire (single crystal α-Al_2O_3) walls at a constant velocity of **20 m/s**. **"Displacement control"**.

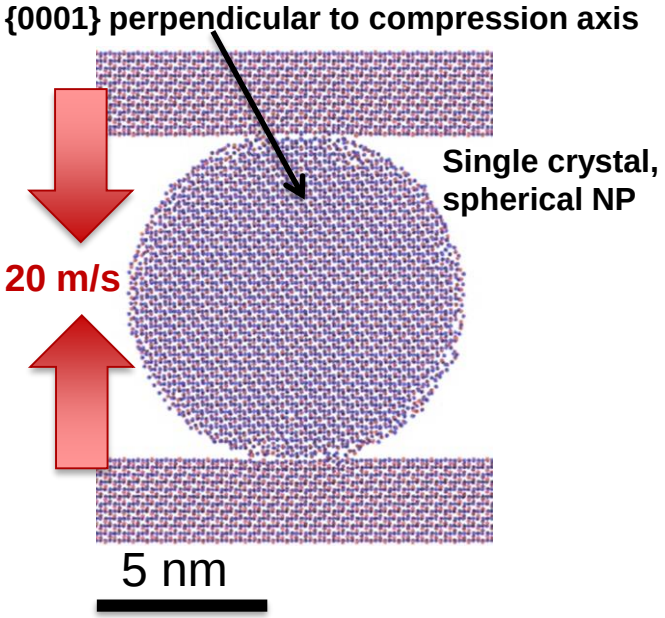

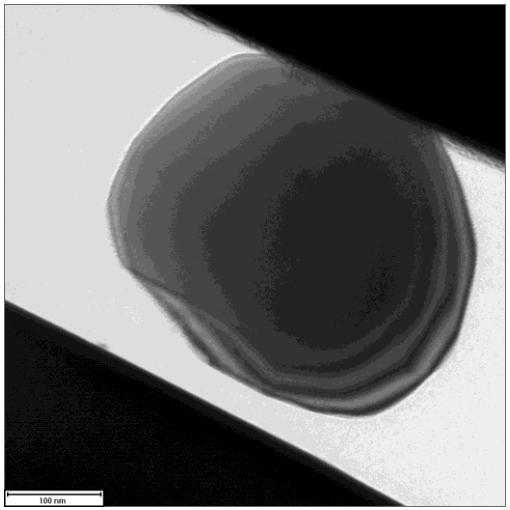

Single crystal, faceted, 300 nm diameter particle

In situ **TEM micro-compression on 0.3μm particle**

[8] Blonski, S. and Garofalini, S. H., *J. Phys. Chem.*, Vol. 100, (1996), pp. 2201-2205.

MD Simulation Results

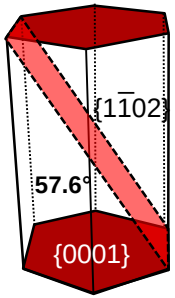

Dislocation nucleation & movement
Dislocation plasticity precedes fracture.

Primary dislocations nucleate at contact points. Then, move through particle on rhombohedral planes

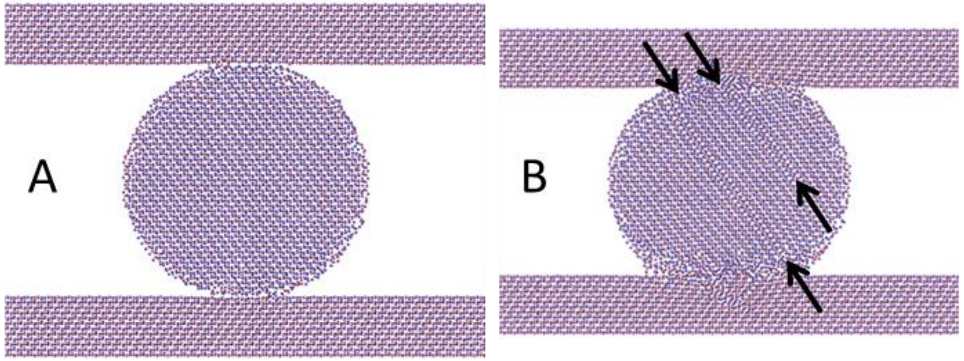

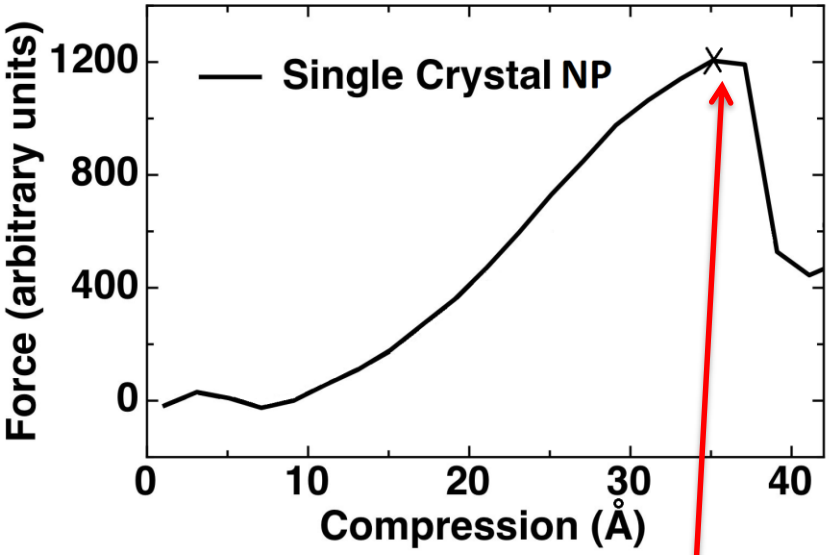

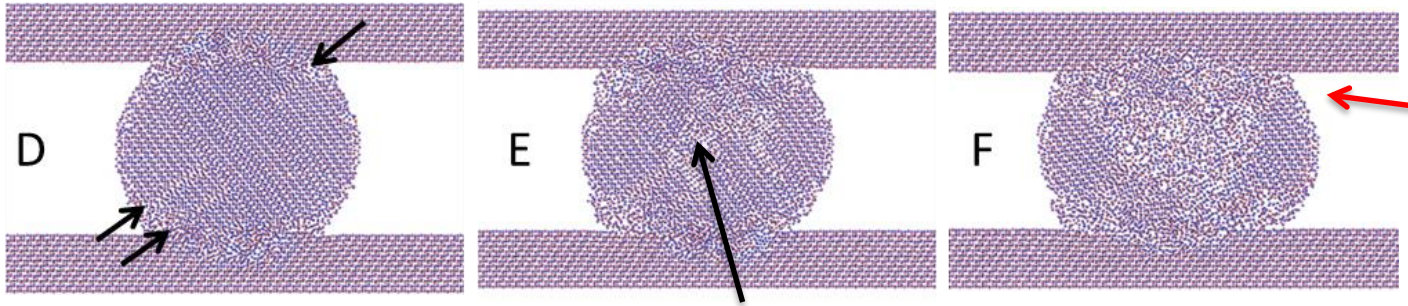

Force drop corresponds to particle fracture

Secondary dislocations nucleate and move through particle on rhombohedral planes, terminating at the primary dislocation planes

Void Initiation

Fracture

MD Simulation Results

Sandia National Laboratories

10 nm diameter, defect-free, single crystal α-alumina, compression axis ⊥ (0001)
20 m/s → dislocation nucleation and glide on Rhombohedral planes then fracture

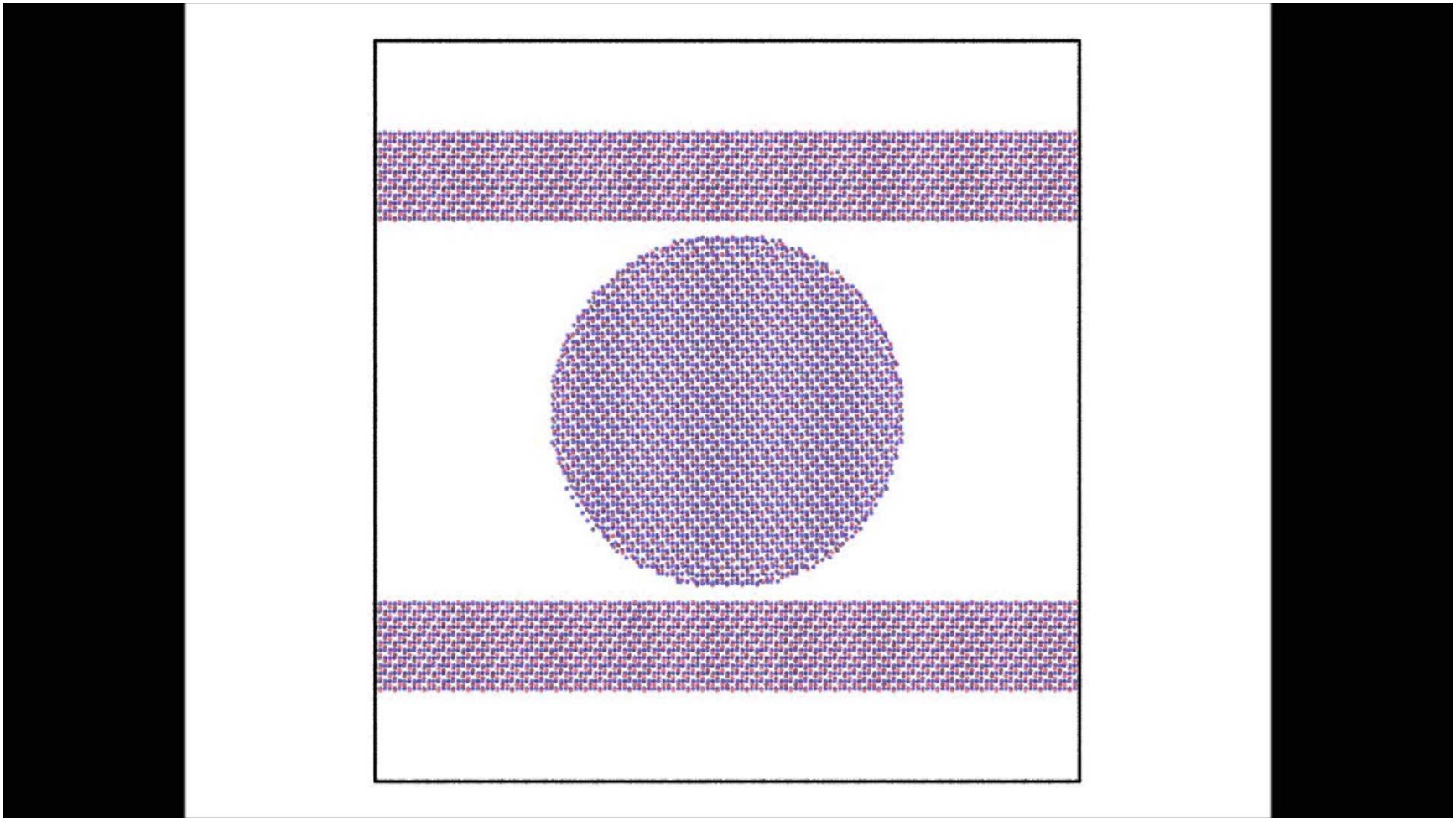

Implications - Compression Study

- Dislocation plasticity precedes fracture in compressed small sapphire particles at RT.
- Need **mobile** dislocations for plastic deformation.
- Use info to inform feedstock preparation, aerosol deposition parameters, and particle-particle bonding in the consolidated coatings.
  - **Ball milling particles introduces dislocations, facilitates plastic deformation, requires less impact energy to consolidate, increases deposition rate.**

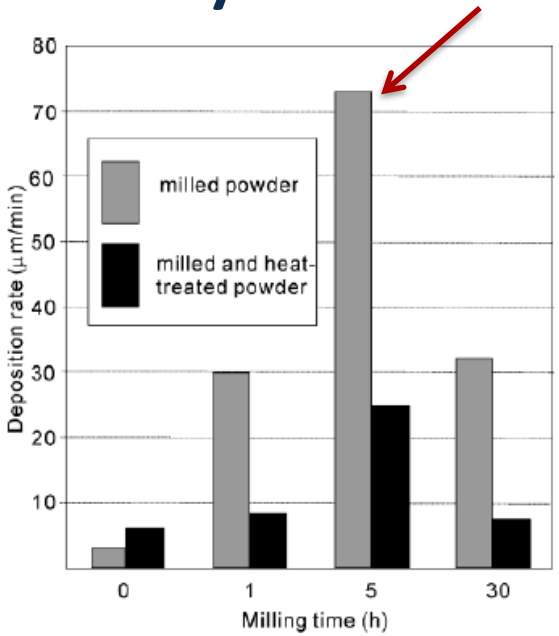

J. Akedo and M. Lebedev. *Jpn. J. Appl. Phys.* Vol. 41 (2002) pp. 6980–6984

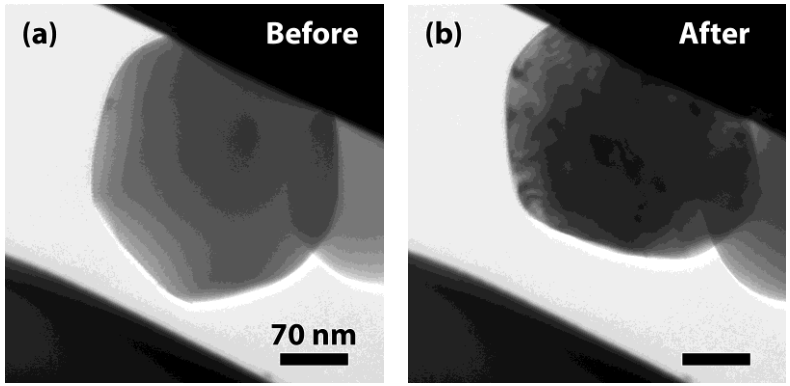

Alumina particle before and after compression.
Note numerous dislocations after compression.

VS.

AD PZT particles are full of dislocations. J. Akedo. J. Am. Ceram. Soc., 89 [6] 1834–1839 (2006)

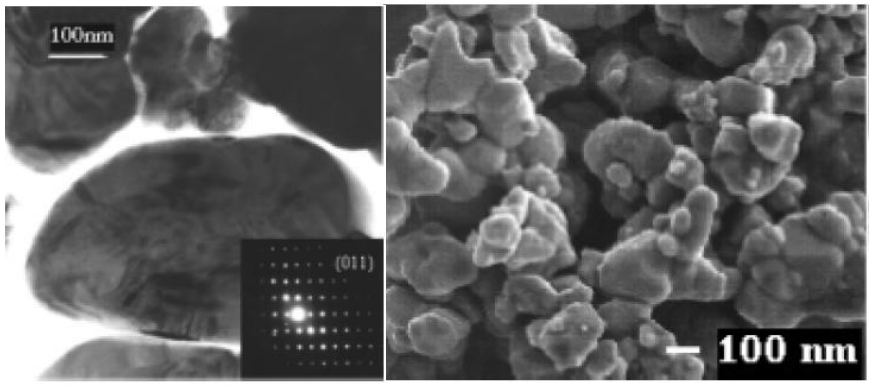

Ball milled PZT feedstock used for Aerosol Depotision
Note numerous dislocations in each particle

Sandia National Laboratories

COMPRESSION STUDY

Quasi-static Loading - Particle compression simulation and experiments.

DEPOSITION STUDY

High Strain-Rate Loading – Single particle impact and coating experiments.

IDENTIFYING DEFORMATION AND CONSOLIDATION MECHANISM

Deposition Study

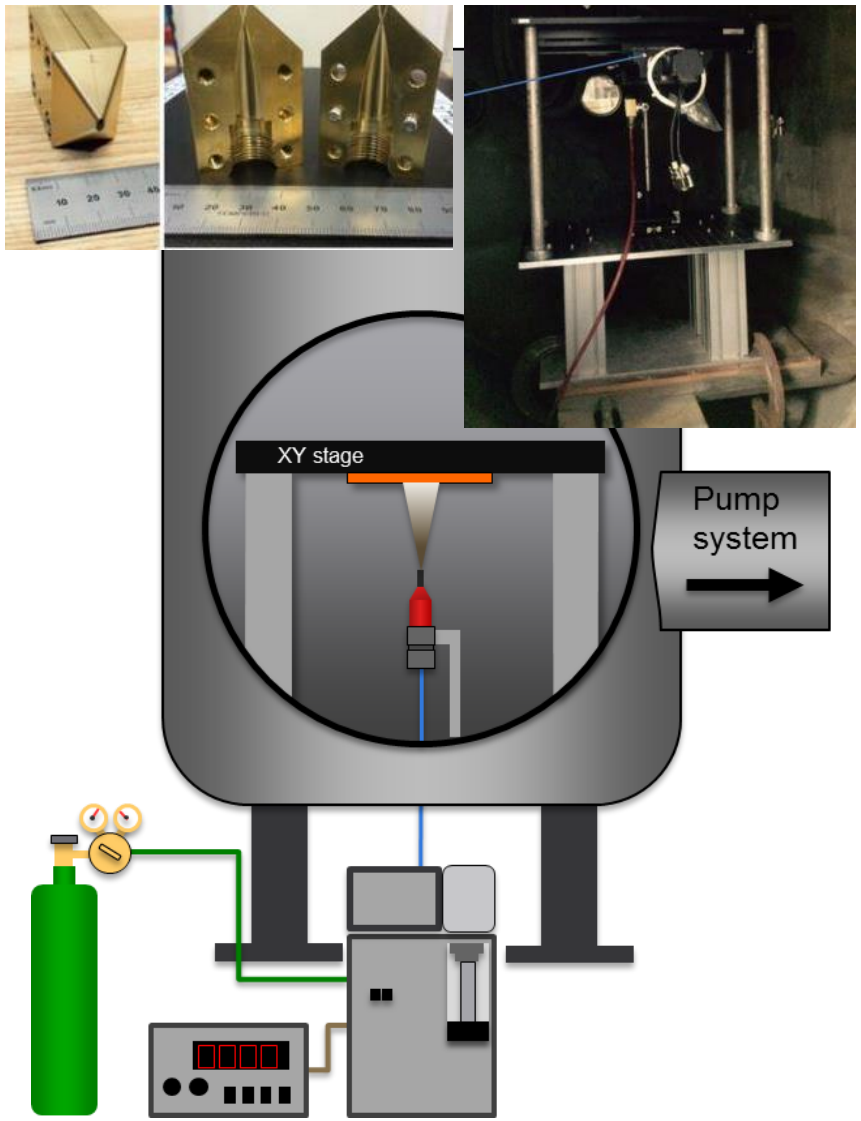

High Velocity Particles

- Pressure differential from the bottle source and the mild vacuum in the chamber.
- Single particle deposition on sapphire
  - 3.0 µm – fractured, fragmented, eroded substrate
  - 0.3 µm – deformed, fractured, adhered to substrate
- Coating deposition on sapphire
  - 0.3 µm – deformed and consolidation

Mechanisms/Building Blocks

- Deformation—dislocation nucleation/slip
- Bonding—mechanical tamping

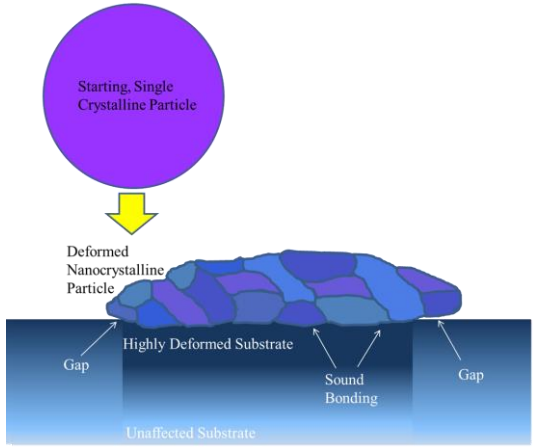

Single Particles Deposition - Alumina

- Sapphire substrate
- Dents – impact from the 3.0µm particles
- Splats – impacted and adhered 0.3µm particles. Diffraction pattern revealed that the splat is polycrystalline.

Carrier Gas = Air
Aerosol Chamber = 20 psig.
Deposition Chamber = 5.8 psi.
Standoff Distance = 5 mm.
Run time = 15 minutes

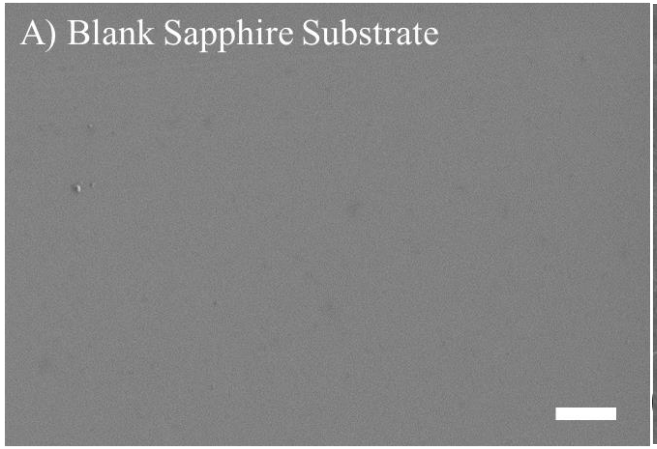

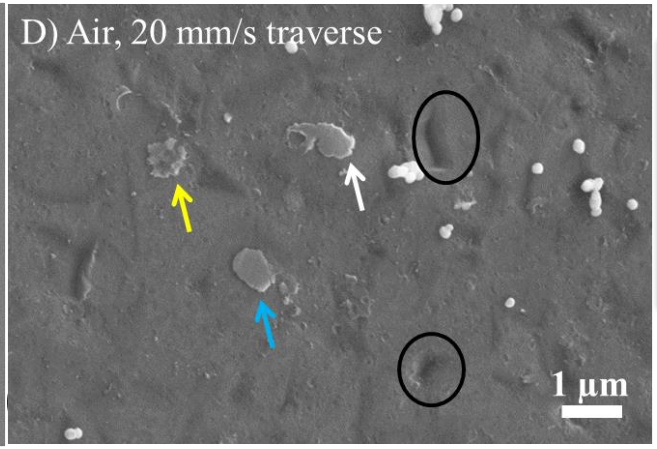

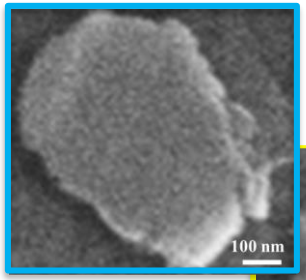

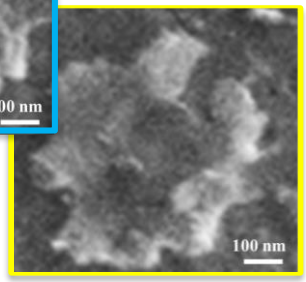

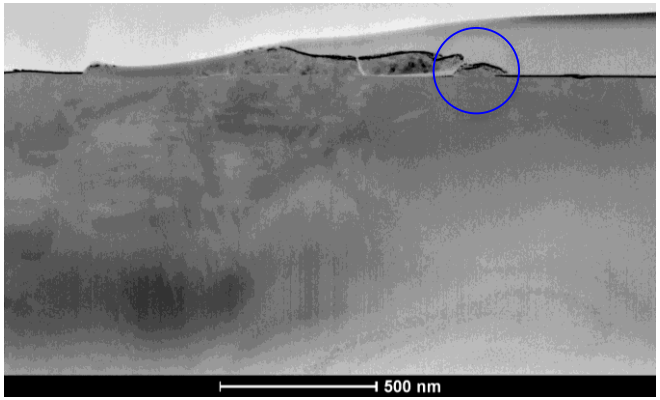

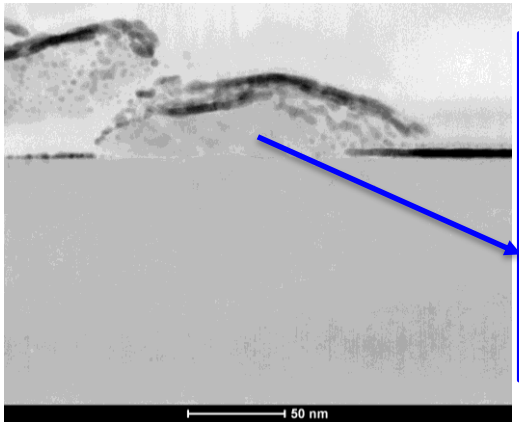

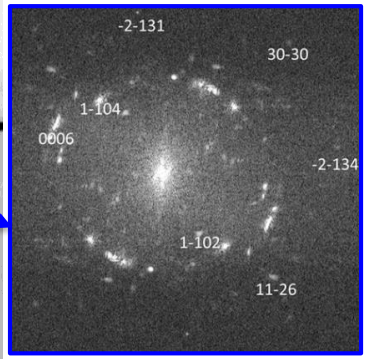

Polycrstalline with orientation spread.

Single Particles Deposition - Alumina

- Bonded area showed a very small disordered layer at the particle/substrate interface.
- Splatted particles deformed and fractured into many subgrains (15-30 nm), without fragmentation.
- Non-bonded area showed <5 nm gap.

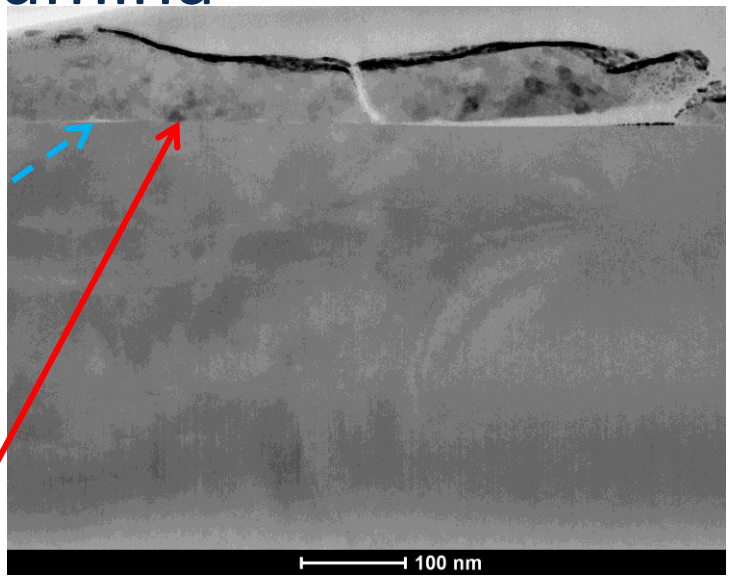

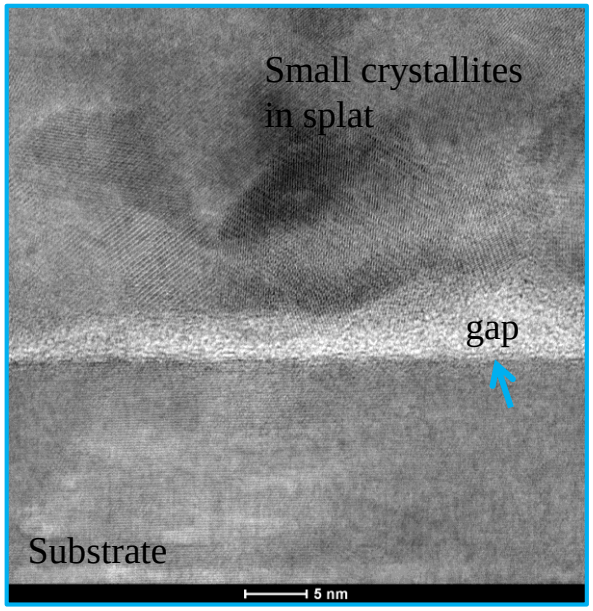

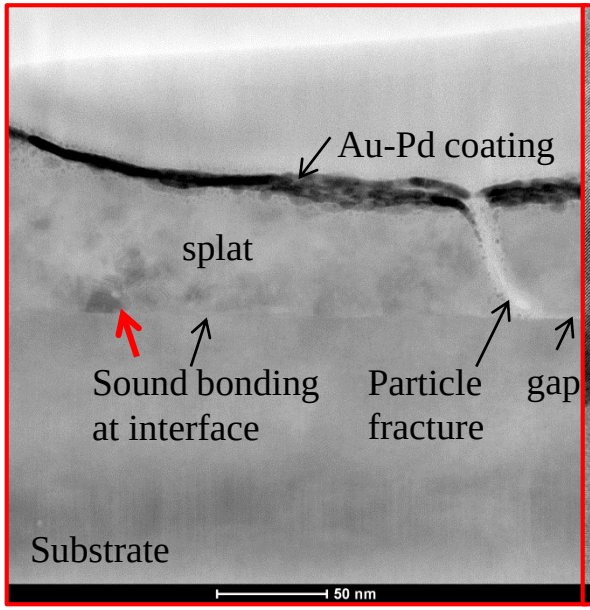

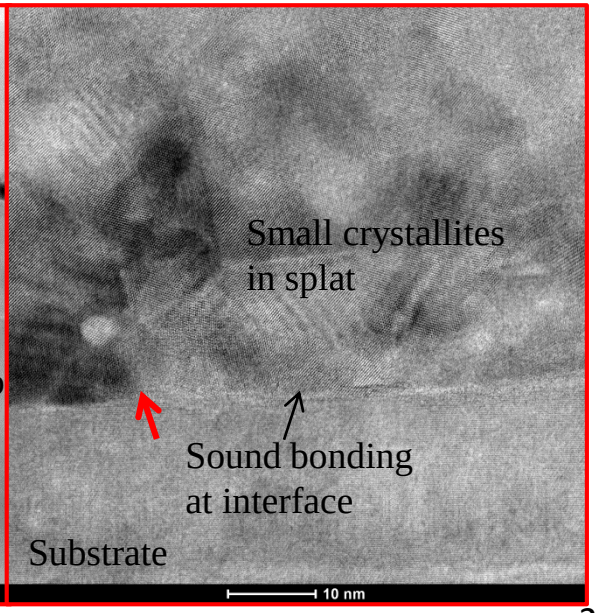

Coating Deposition - Alumina

- Interface almost indistinguishable
- Nanocrystalline coating ~100-150nm thick.
- The kinetic energy facilitated deformation and chemi-mechanical alumina particle-sapphire substrate bonding.
- “Tamping Effect” [1-4].

Carrier Gas = He
Aerosol Chamber = 25 psig.
Deposition Chamber = 0.05 psi.
Standoff Distance = 5 mm.
Run time = 15 minutes

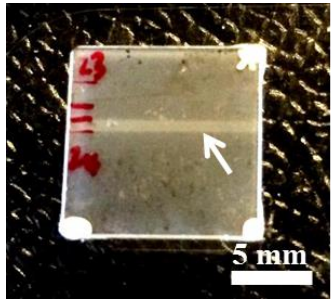

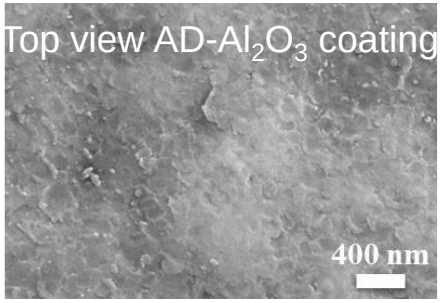

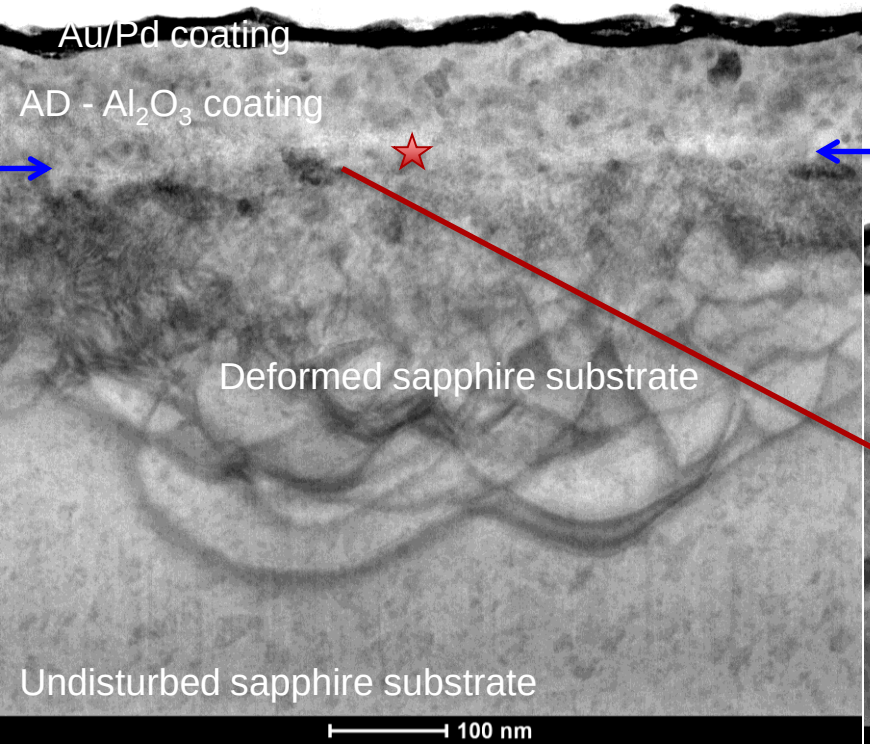

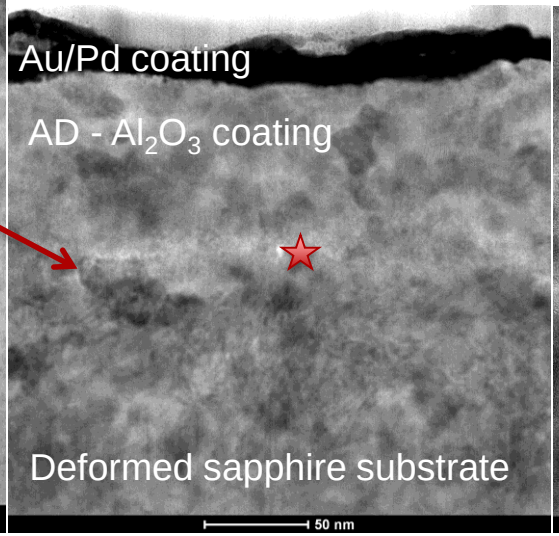

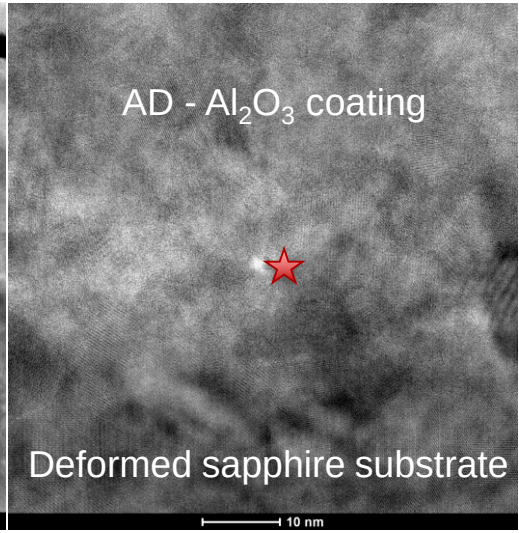

[1] H. Park, et al. *JTST*, 2013:**22**;882. [2] Y.-Y. Wang et al. *JTST*, 2010:**19**;1231
[3] F. Cao, et al. *JTST*, 2013:**22**; 1109 [4] S.-Q. Fan, et al. *JTST*, 2006:**15**;513

Compression & Deposition Studies

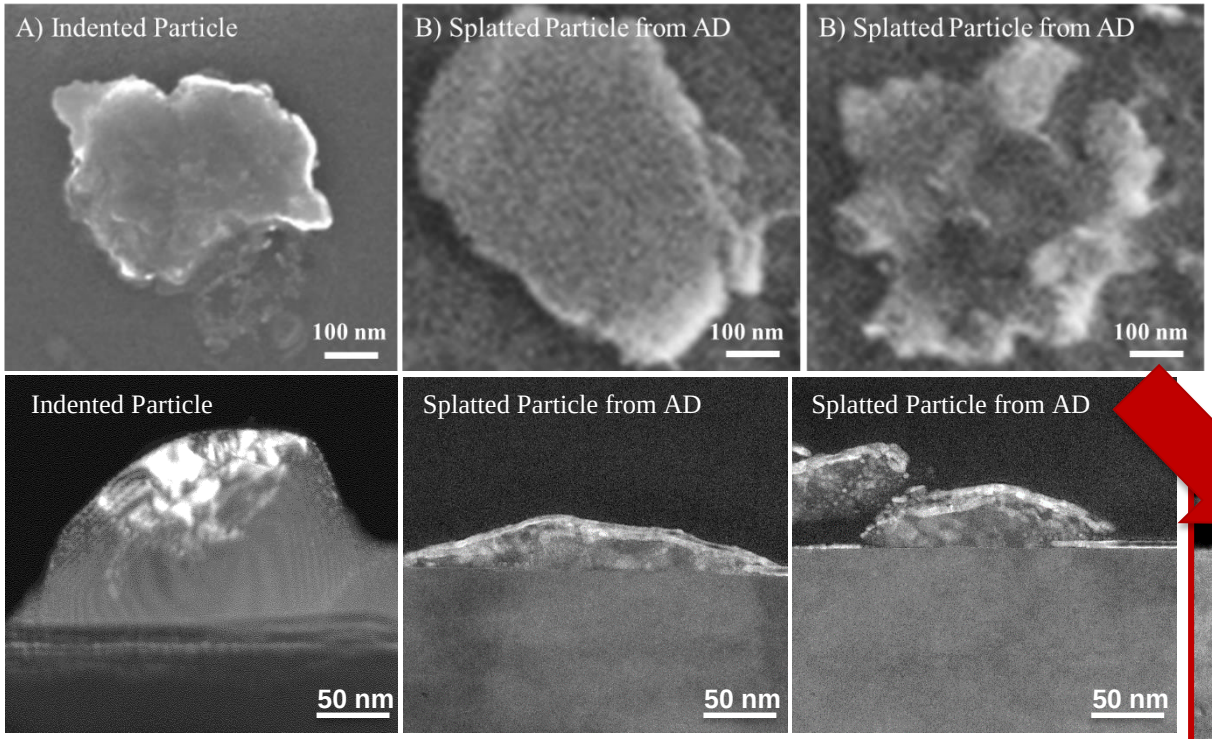

- Observed similar microstructural characteristics in the indented particles and the splatted particles.
- "Tamping" from subsequent impacting particles build up dense coating.

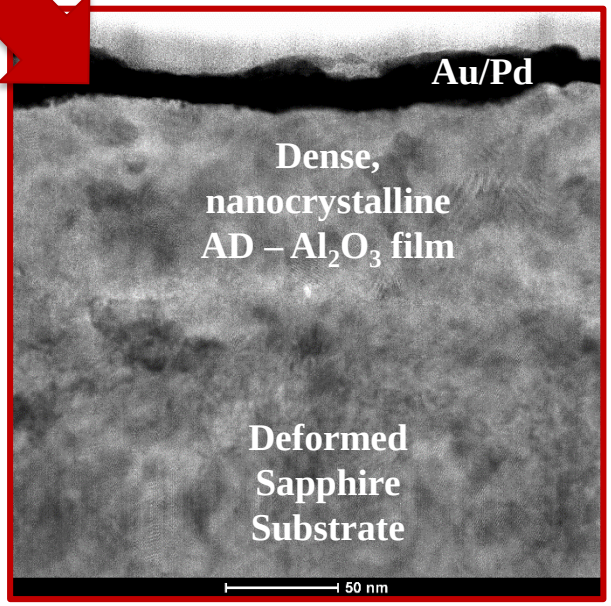

In both quasi-static and high strain-rate loadings, 0.3 μm Al_2O_3 feedstock particles underwent plastic deformation. Characteristics include:

- dislocation nucleation and slip
- shape change
- fracture into nanocrystals (15-30 nm)
- polycrystalline with mosaicity

RT Deformation & Bonding Mechanisms

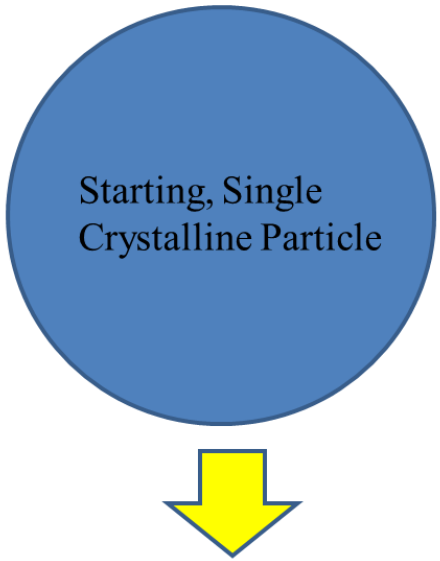

RT Deformation & Bonding Mechanisms

Sandia National Laboratories

Kinetic Energy converted to absorbed strain energy, providing

- Dislocation plasticity to deform particle
- Fracture - nanocrystalline formation in particle
- Chemi-mechanical bond between alumina particle-sapphire substrate

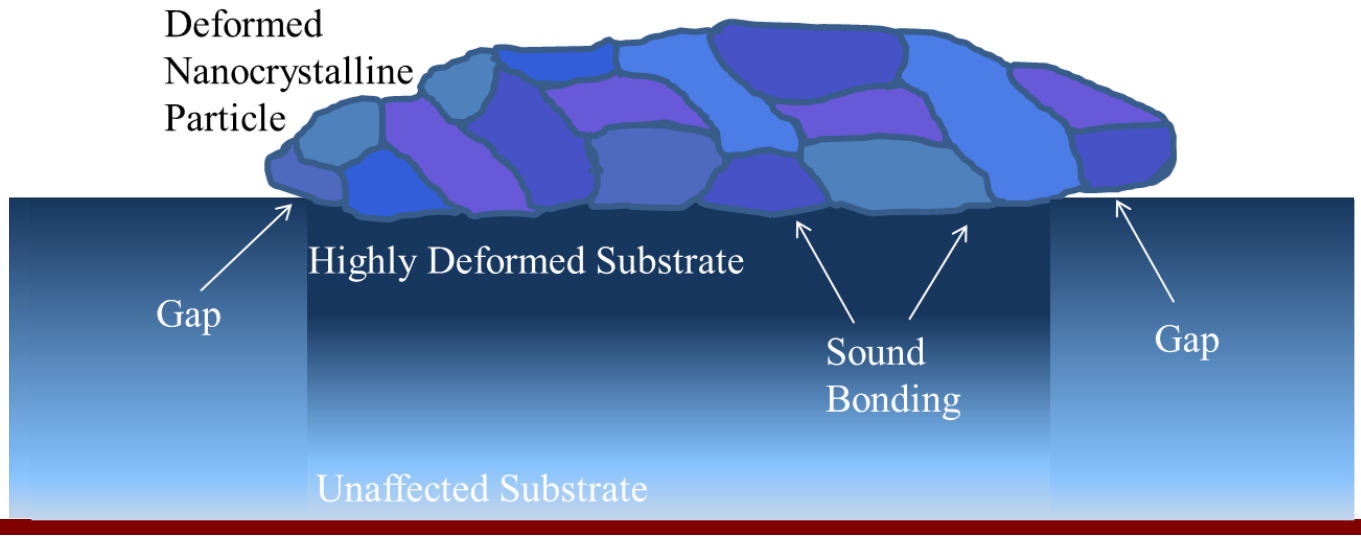

RT Deformation & Bonding Mechanisms

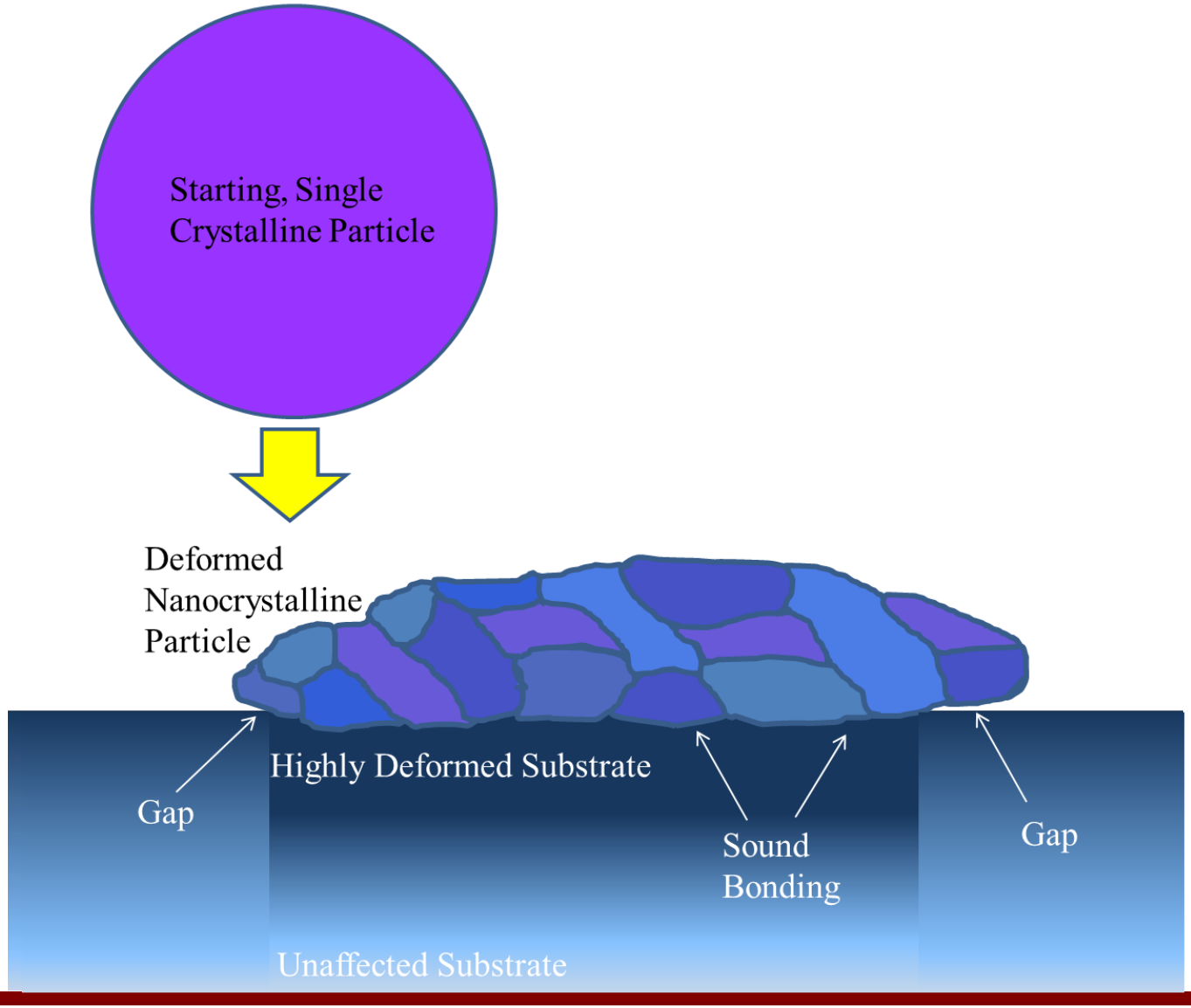

RT Deformation & Bonding Mechanisms

Sandia National Laboratories

Subsequent impacting particle imparts sufficient energy to

- Further deform splatted particle
- Provide further bond formation between splatted particle-substrate from “tamping effect”
- Compaction and densification of deposited coating from “tamping effect”

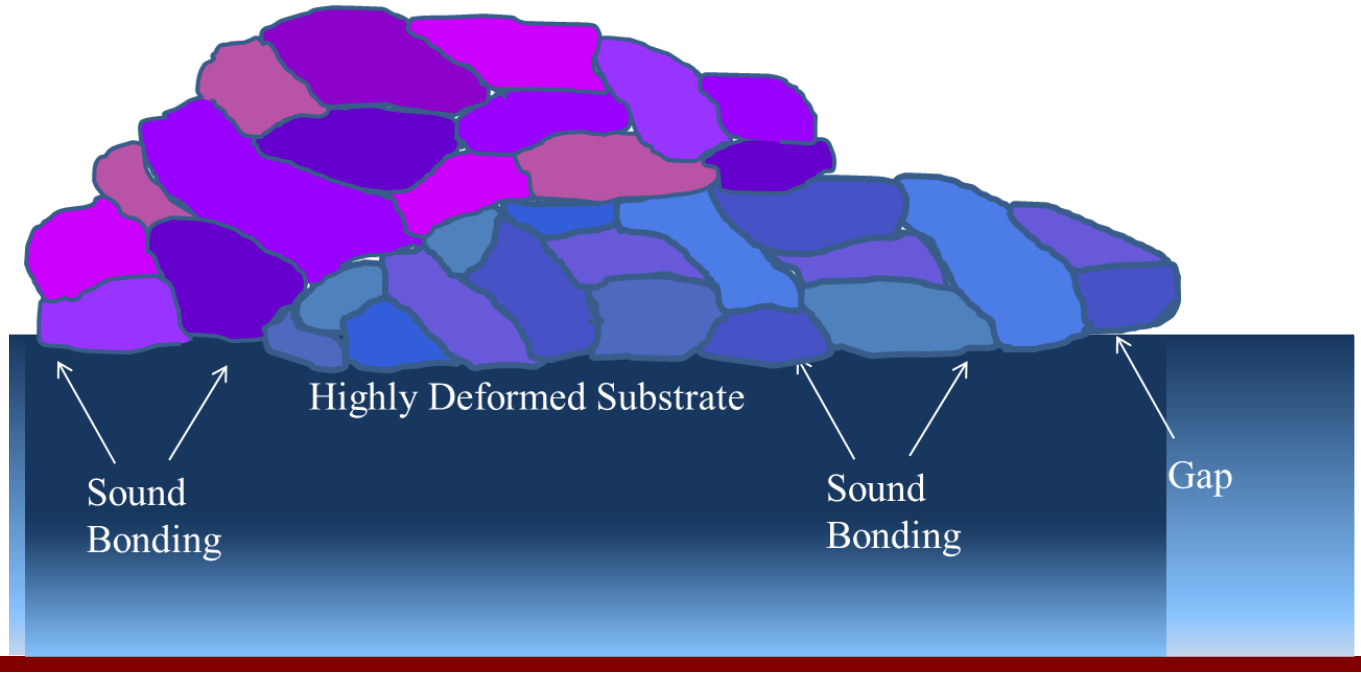

Special Materials Consolidation, Electrical Interconnects, Micro-devices

INTEGRATIONS & APPLICATIONS

Current Development

FY14-16 Initial Demonstration and Process Development → Technology Maturation

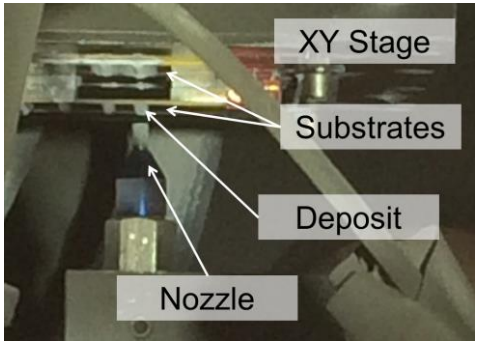

- Room temp. consolidation

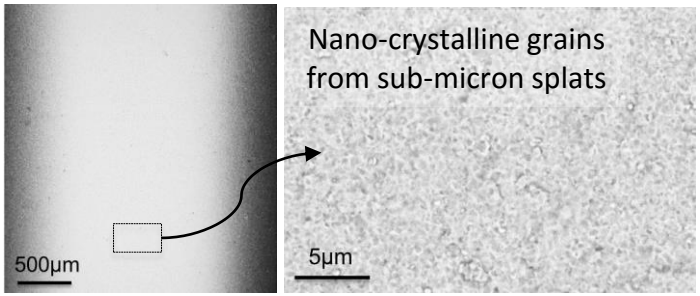

- Processing parameter exploration and SEM imaging

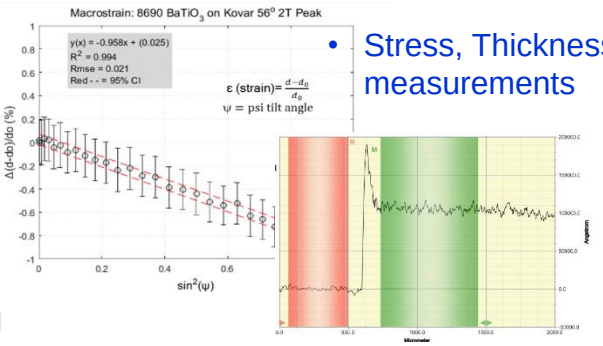

- Stress, Thickness measurements

FY16 Opportunities - Expanding suite of materials

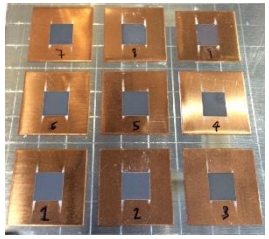

AD – $BaTiO_3$ on Cu Substrates

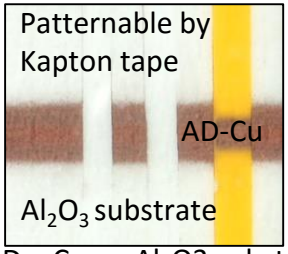

AD – Cu on Al_2O3 substrate

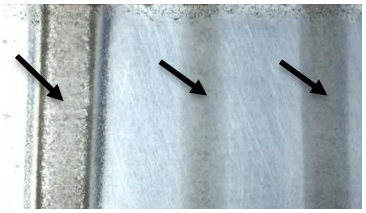

AD- carbide compound

AD - Ni on Glass Substrate

- More matured AD process.
- Metallic, ceramic, "brittle" compound coatings.

FY16 Opportunities – Development for Potential Devices and Applications

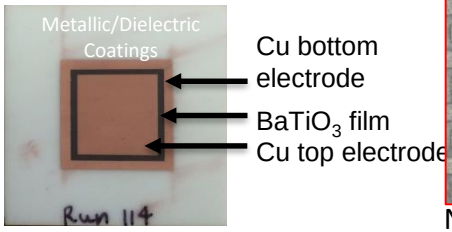

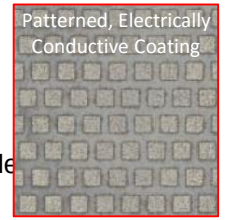

Ni interconnects

Heat Treatment – process/microstructure/properties

- Nanocrystalline grain size (10-30 nm)
- Defects in coatings
- Coating compressive residual stress

Applications

- Electrical interconnects
- High dielectric capacitors
- Special coatings for thermal protection

Towards High Dielectric Capacitors

Goal: Deposit high K dielectrics on base metals at room temp → Capacitors

- Aerosol deposited, 6um thick
- BaTiO3 and (Bi,Na)TiO_3
- High temp induced Bi vaporization
  - Vacancies of Bi and O formation
- Temp induced crystallographic Phase Transition changes properties
  - Dielectric (capacitor)
  - Piezoelectric (actuator)

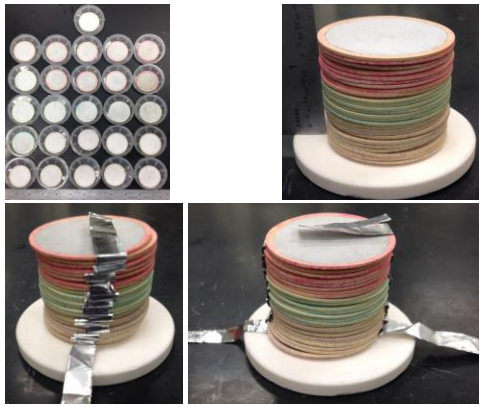

Brown-Shaklee et al.'s SNL Dev – Office of Electricity - High Temperature Reliable Dielectrics for DC Link Capacitors

www.globalsources.com

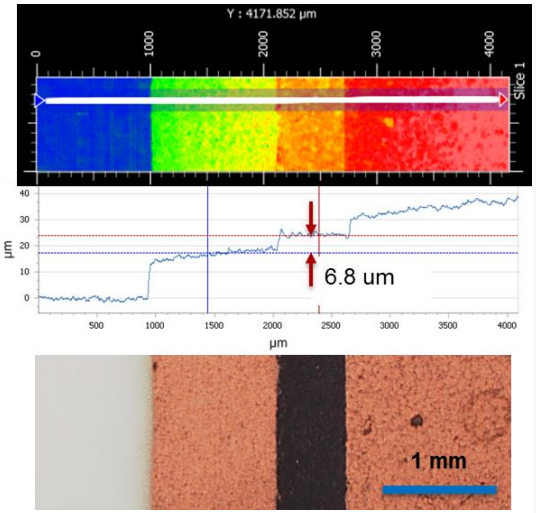

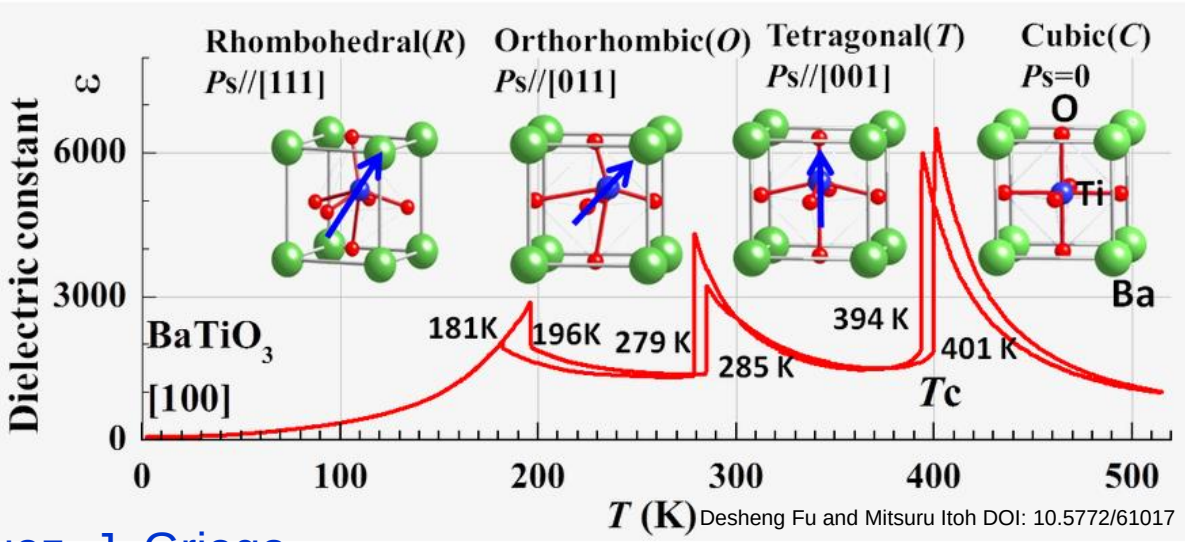

Desheng Fu and Mitsuru Itoh DOI: 10.5772/61017

H. Brown-Shaklee, M. Rodriguez, J. Griego

Towards High Dielectric Capacitors

Goal: Deposit high K dielectrics on base metals at room temp → Capacitors

- Aerosol deposited, 6um thick
- XRD phase and strain measurement
- ~1% in-plane strain → 1.3 GPa stress.

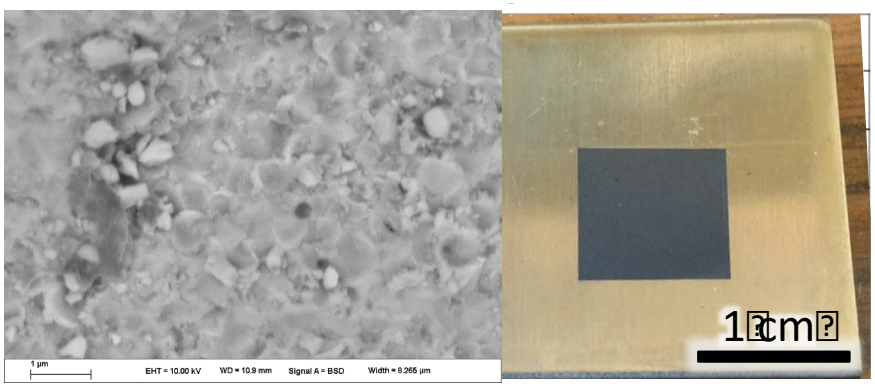

· Error bars were determined via peak profile fit results from $BaTiO_3$ (211) peak
· The magnitude of the error bars are a factor of the broadened peaks
· The 95% confidence interval bands are factors of the fit-type (linear polynomial curve)

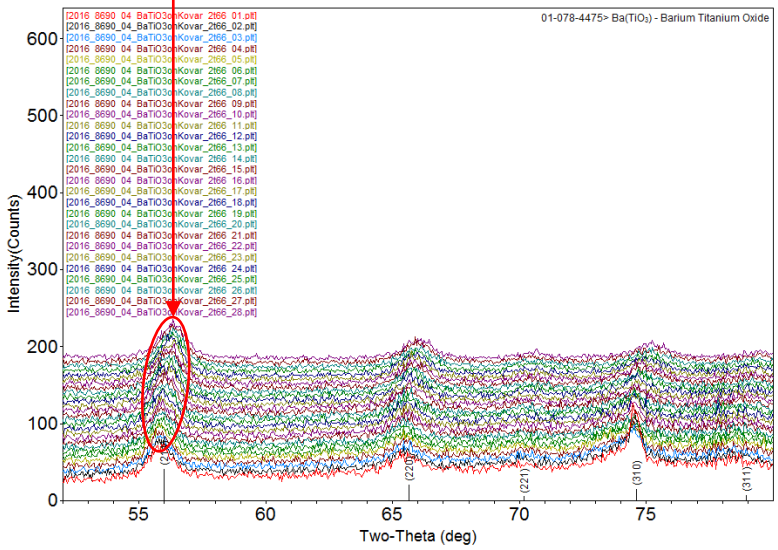

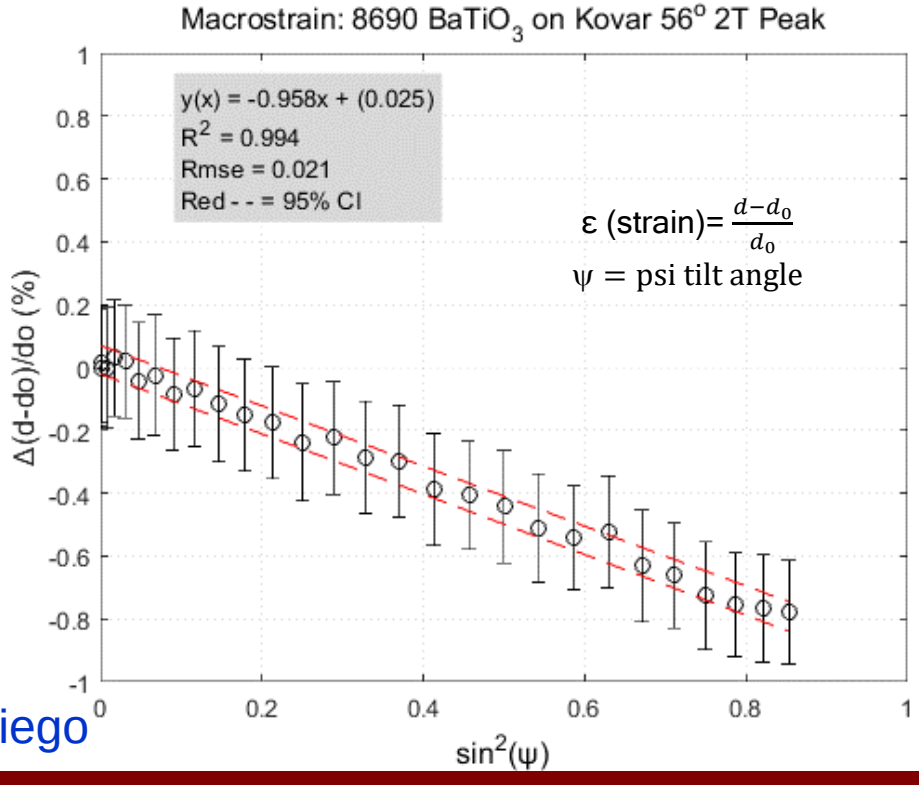

H. Brown-Shaklee, M. Rodriguez, J. Griego

Towards High Dielectric Capacitors

Goal: Deposit high K dielectrics on base metals at room temp → Capacitors

- Aerosol deposited, 6um thick
- XRD phase and strain measurement
- ~1% in-plane strain → 1.3 GPa stress.
- Future work: deposit Bi-containing $BaTiO_3$ dielectrics (BNT, etc.) in the same manner.
- Ability to deposit Bi-based dielectrics at room temperature will further enable the design, fabrication, and testing of high capacity devices without the use of precious metals.
- Future work – understand how film residual strain and heat treatment affect leakage current density / polarization loop / other properties.

Suzuki, M. et al. J Ceram Soc Jpn 118 [10] 899-902 2010

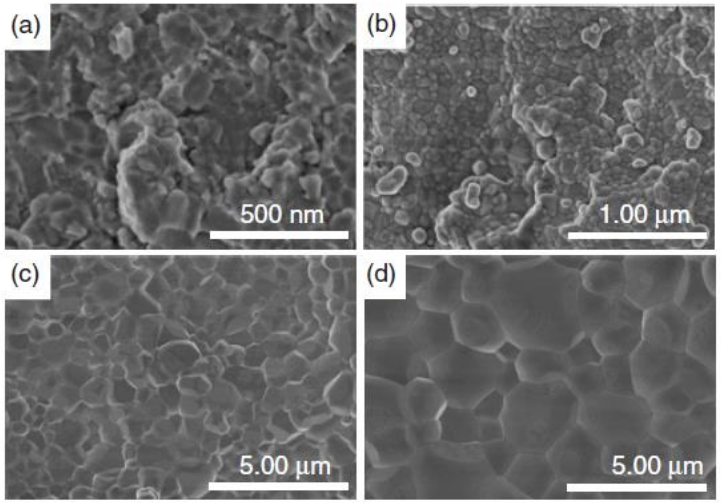

Fig. 2. Microstructure observation by SEM images of the BNT ceramic films (a) of as-deposition films, (b) annealed at 800°C, (c) at 1000°C and (d) at 1100°C.

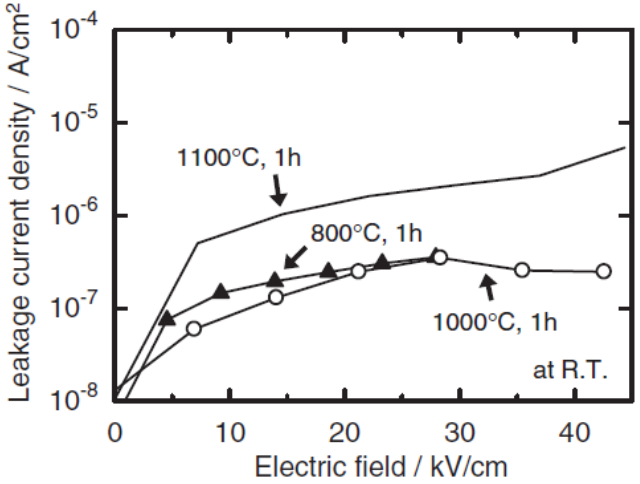

Fig. 4. Leakage current properties measured at 25°C for the BNT ceramic films annealed at 800, at 1000, and at 1100°C.

H. Brown-Shaklee, M. Rodriguez, J. Griego

Conclusions

- AD Feedstock – Submicron particles plastic deformation
  - Experiments and Simulations confirmed dislocation nucleation, slip, fracture without fragmentation
- Tamping Effect – bonding
  - allow anchor layer to form complete bond to the substrate.
  - Further deform, fracture, and mechanically bond the arriving particles to the already deposited particles.
- Room temperature plasticity in ceramics at small length scale gave insights into future development of alternative ceramic forming technology such as aerosol deposition (AD) and high strength/high toughness functional ceramics.
- Future work = investigating heat treatment effect on process-microstructure-property relationship.

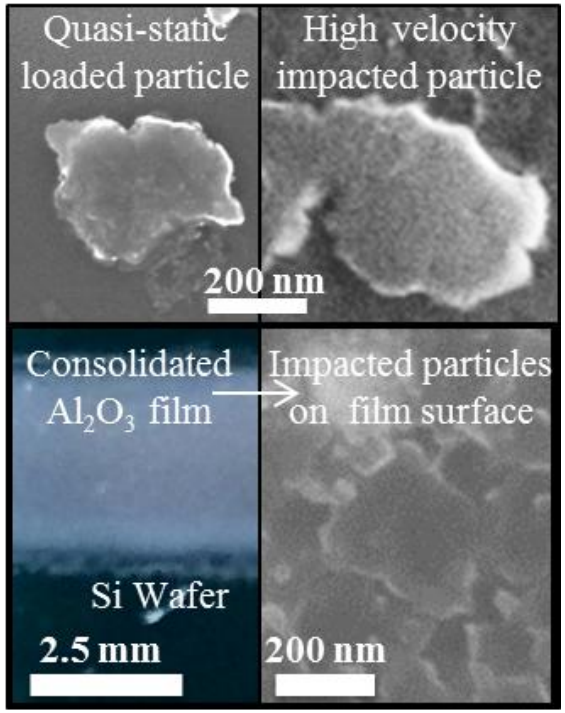

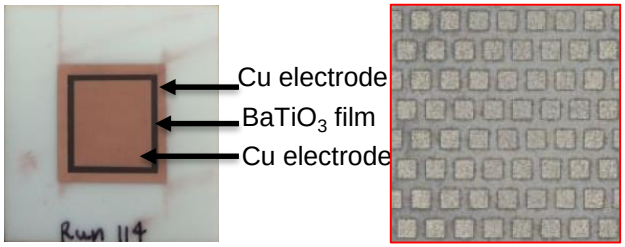

The knowledge gained from this work provides a strong foundation to mature the Sandia aerosol deposition process for fabricating ceramic films on metallic, glass, and plastic substrates at RT.

References

1A.R. Beaber, J.D. Nowak, O. Ugurlu, W.M. Mook, S.L. Girshick, R. Ballarini, W.W. Gerberich, *Philos. Mag.*, **91**, 1179 (2011).
2W.W. Gerberich, J. Michler, W.M. Mook, R. Ghisleni, F. Östlund, D.D. Stauffer, and R. Ballarini, *J. Mater. Res.*, **24**, 898 (2009).
3W.W. Gerberich, W.M. Mook, M.J. Cordill, C.B. Carter, C.R. Perrey, J.V. Heberlein, and S.L. Girshick, *Int J Plasticity*., **21**, 2391 (2005).
4F. Östlund, K. Rzepiejewska-Malyska, K. Leifer, L.M. Hale, Y. Tang, R. Ballarini, W.W. Gerberich, and J. Mitchler, *Adv. Funct. Mater*., **19**, 2439 (2009).
5G. Xu and C. Zhang, *J. Mech. Phys. Solids*, **51**, 1371 (2003).
6P.R. Howie, S. Korte, and W.J. Clegg, *J. Mater. Res.*, **27**, 141 (2012).
7W.M. Mook, C. Niederberger, M. Bechelany, L. Phillippe, and J. Michler, *Nanotechnology*, **21**, 05570 (2010).
8H. Bei, S. Shim, G.M. Pharr, and E.P. George, *Acta Mater*., **56**, 4762 (2008).
9F. Östlund, P.R. Howie, R. Ghisleni, S. Korte, K. Leifer, W.J. Clegg, and J. Michler, *Philos. Mag*. **91**, 1190 (2011).
10S. Montagne, S. Pathak, X. Maeder, and J. Michler, *Ceram Int*. **40**, 2083 (2014).
11M.D. Uchic, D.M. Dimiduk, J.M. Florando, and W.D. Nix, *Science*, **305**, 986 (2004).
12D.M. Dimiduk, M.D. Uchic, and T.A. Parthasarathy, *Acta Mater*., **53**, 4065 (2005).
13J.R. Greer, W.C. Oliver, and W. Nix, *Acta Mater.*, **53**, 1821 (2005).
14O.A. Ruano, J. Wadsworth, and O.D. Sherby, *Acta Mater*. **51**, 3617 (2003).
15A. Dominguez-Rodriguez, F. Gutierrez-Mora, M. Jimenez-Melendo, J.L. Routbort, and R. Chaim, *Mater. Sci. Engr. A*. **302**, 154 (2001).
16J. Akedo and H. Ogiso, *JTST*, **17**, 181 (2008).
17J. Akedo. *JTTEE5*, **17**, 181 (2007).
18J. Akedo, *J. Am. Ceram. Soc*., **89**, 1834 (2006).
19Y. Imanaka, N. Hayashi, M. Takenouchi, and J. Akedo, *Proc. of Ceramic Interconnect and Ceramic Microsystems Technologies*, 2006.
20Y. Imanaka, N. Hayashi, M. Takenouchi, and J. Akedo, *J. Euro. Ceram. Soc*. **27**, 2789 (2007).
21Y. Kawakami, H. Yoshikawa, K. Komagata, and J. Akedo, *J. Crys. Growth*. **275**, el295 (2005).
22J. Akedo and M. Lebedev, "Piezoelectric Properties and Poling Effect of Pb(Zr, Ti)O_3 Thick Films Prepared for Microactuators by Aerosol Deposition," *Appl. Phys. Lett*. 77, 2000, p. 1710.
23S. Sugimoto, T. Maeda, R. Kobayashi, J. Akedo, M. Lebedev, and K. Inomata, *IEEE Trans. Magnetics.* **39**, 2986 (2003).
24S. Sugimoto, T. Maki, T. Kagotani, J. Akedo, and K. Inomata, *J. Magn. Magn. Mater*. **290-291**, 1202 (2005).
25H. park, J. Kwon, I. Lee, and C. Lee, *Scripta Materialia*, **100**, 44 (2015).
26M. Schubert, J. Exner, and R. Moos, *Materials,* **7**, 5633 (2014).
27D.W. Lee and S.M. Nam, *J. Ceram. Process. Res*. **11**, 100 (2010).
28S.H. Cho and Y.J. Yoon, *Thin Solid Films*, **547**, 91 (2013).
29Y.J. Heo H.T. Kim, K.J. Kim, S. Nahm, Y.J. Yoon, and J. Kim, *Appl. Therm. Eng*. **50**, 799 (2013).
30J. Exner, P. Fuierer, and R. Moos, *J. Am. Ceram. Soc*. **98**, 717 (2015).
31W.E. Lee and K.P.D. Lagerlof, *J. Electron Microscopy Technique*. **2**, 247 (1985).
32J.D. Snow and A.H. Heuer , *J. Am. Ceram. Soc.*, **56**, 153 (1973).
33M.L. Kronberg , *Acta Metall.*, **5**, 508 (1957).
34A.H. Heuer , *Phil. Mag*., **13**, 379 (1966).
35*Deformation of Ceramic Materials* edited by R.C. Bradt and R.E. Tressler (Plenum Press, New York, 1975)
36N.I. Tymiak and W.W. Gerberich, *Phil. Mag*., **87**, 5143 (2007).
37N.I. Tymiak and W.W. Gerberich, *Phil. Mag*., **87**, 5169 (2007).
38R. Nowak, T. Sekino, and K. Niihara, *Phil. Mag. A*, **74**, 171 (1996).
39J.D. Clayton, *Proc. Of the Royal Soc. A.,* **465**, 307 (2009).
40E.R. Dobrovinskaya, L.A. Lytvynov, and V. Pishchik, *Sapphire* (Springer, Boston, MA 2009).
41K.P.D. Lagerlof, A.H. Heuer, J. Castaing, J.P. Riviere, and T.E. Mitchell, *J. Am. Ceram. Soc.*, **77**, 385 (1994).
42A. Nakamura, T. Yamamoto, and Y. Ikuhara, *Acta Mater*., **50**, 101 (2002).
43T. Geipel, K.P.D. Lagerlof, P. Pirouz, and A.H. Heuer, *Acta Matall. et Mater*., **42**, 1367 (1994).
44K. Hattar, D.C. Bufford, and D.L. Buller, *Nuclear Instruments and Methods in Physics Research B*. **338**, 56 (2014).
45K. Zhen, C. Wang, Y.-Q. Cheng, Y. Yue, X. Han, Z. Zhang, Z. Shan, S.X. Mao, M. Ye, Y. Yin, and E. Ma. Nature Communications | 1:24 | DOI: 10.1038/ncomms1021
46W.M. Mook, J.D. Nowak, C.R. Perry, C.B. Carter, R. Mukherjee, S.L. Girshick, P.H. McMurry, and W.W. Gerberich, *Phys Rev B*, 75, 2007, pp. 214112-1-10.
47*Materials Science and Engineering Serving Society* edited by R.P.H. Chang, R. Roy, M. Doyama, and S. Somiya. (Elsevier Science, The Netherlands, 1998).
48D.D. Stauffer, A. Beaber, A. Wagner, O. Ugurlu, J. Nowak, K. Andre Mkhoyan, S. Girshick, and W.W. Gerberich, Acta Mater., **60**, 2471 (2012).

Thank you, for your attention!

Pylin Sarobol –

psarobo@sandia.gov

Coatings and Additive Manufacturing

Sandia National Laboratories

Sandia National Laboratories

BACK UP SLIDES

Ceramic Particle RT Deformation - Sapphire

- Deformation behavior influenced by *number of internal defects*, temperature, crystal orientation/size. Numbers of pre-existing (immobile) defect scale with size.
- In situ SEM/TEM micro-compression and Molecular Dynamics Simulations

Proposed

	Micron	Sub-micron
# Pre-existing Defects	High	Moderate
Energy Density Input	Low	Moderate
Governing Mechanism(s)	Fracture	Plasticity + Fracture
Response to Compression	Crack initiation & Propagation	Dislocation nucleation, slip, crack initiation & propagation
Compression Testing	SEM	SEM and TEM

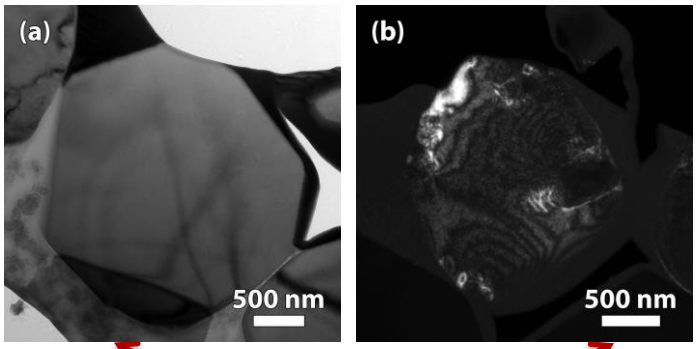

3.0μm Highly Defective

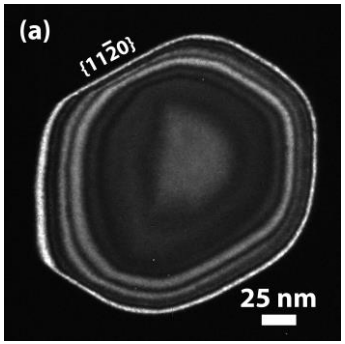

0.3μm Nearly Defect Free

- Infeasible (long computing time) to perform molecular dynamics simulations on size >0.05μm
- 'smaller' particles (0.3μm) are nearly defect-free, and 'larger' particles (3.0μm) contain immobile defects that serve as crack nucleation sites.
- Circumvented the size limitation of our models by simulating similar sized (10 nm) nanoparticles (NPs) that were either
  - single crystal
  - contained a grain boundary (GB) as an initial immobile defect.
- This approach still enables the study of NP deformation/fracture in computationally-feasible systems.

Ceramic Particle RT Deformation - Alumina

- Deformation behavior influenced by *number of internal defects*, temperature, crystal orientation/size. Numbers of pre-existing (immobile) defect scale with size.
- In situ SEM/TEM micro-compression and Molecular Dynamics Simulations

Proposed

	Micron	Sub-micron	Single Crystal Nano	Bicrystal Nano
# Pre-existing Defects	High	Moderate	None	Grain Boundary
Energy Density Input	Low	Moderate	High	Low
Governing Mechanism(s)	Fracture	Plasticity + Fracture	Plasticity	Fracture
Response to Compression	Crack initiation & Propagation	Dislocation nucleation, slip, crack initiation & propagation	Dislocation nucleation, Slip	Crack initiation & propagation
Compression Testing	SEM	SEM and TEM	MD Simulation	MD Simulation

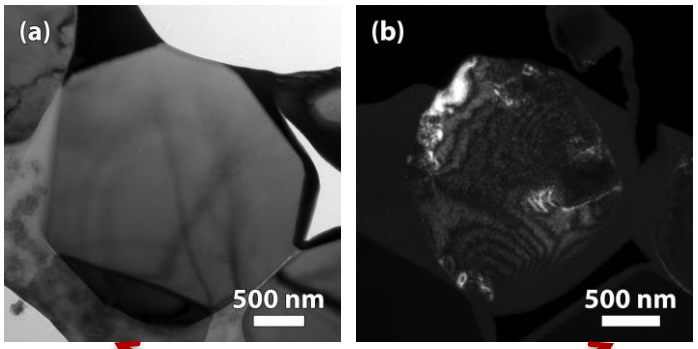

3.0μm Highly Defective

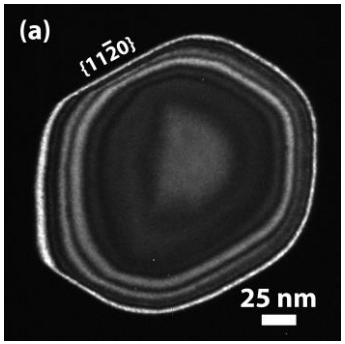

0.3μm Nearly Defect Free

Spherical Particles

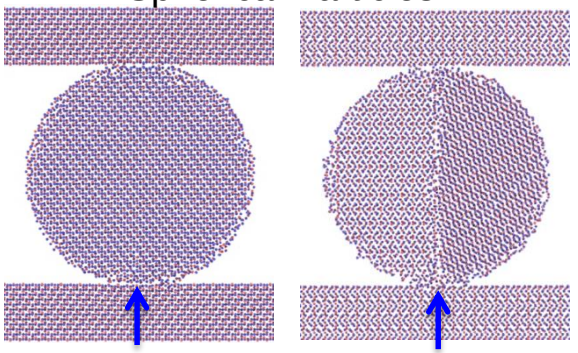

10 nm Defect Free

10 nm with a GB

Ex Situ SEM observation – 0.3 µm

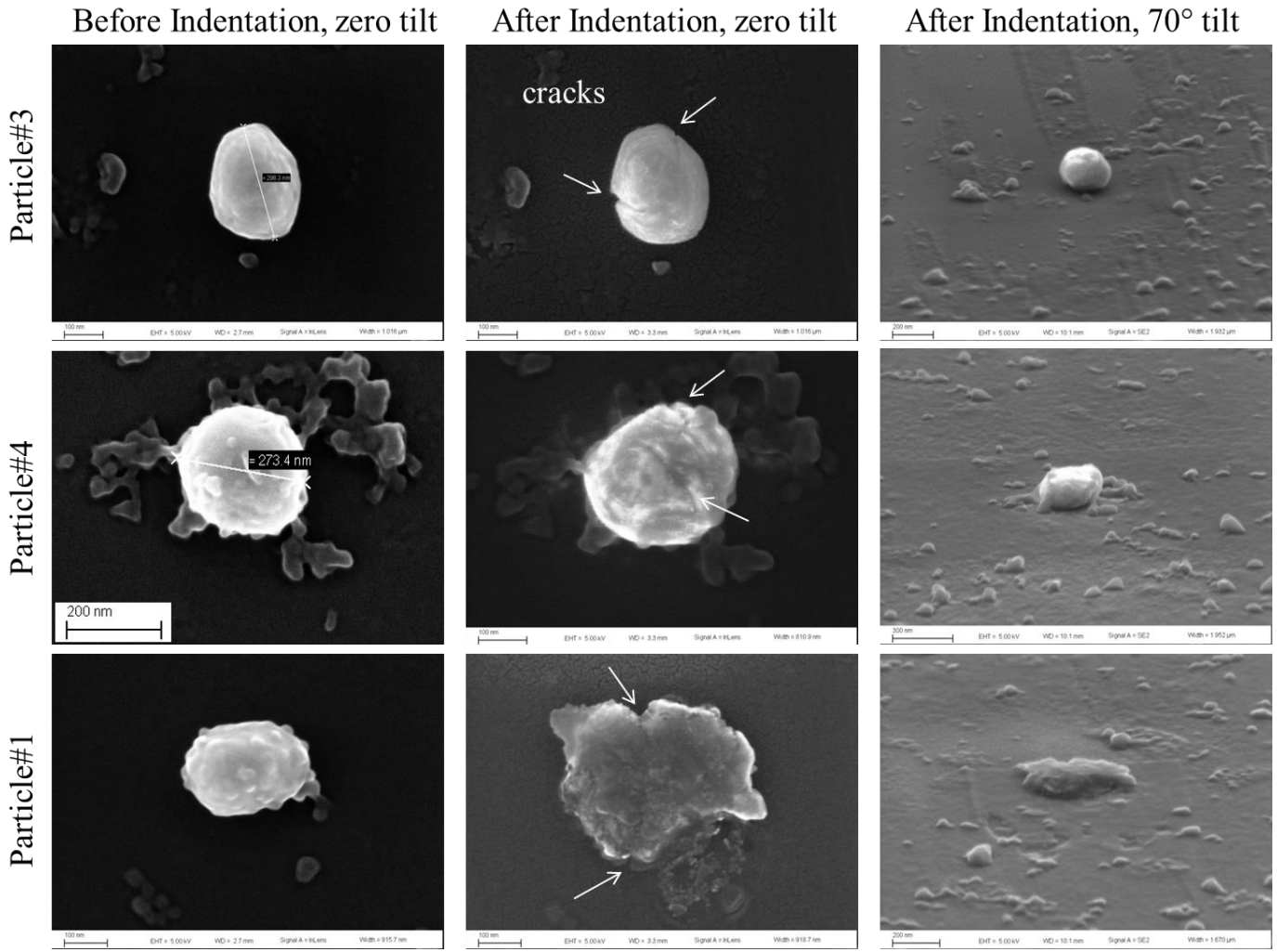

~307 µN
Max load

~420 µN
Max load

Extreme
Loading

Different deformation behavior and load at first fracture may differ from particle-to-particle due to orientation differences and different pre-existing defect densities. However, overall, the sub-micron sized alumina particles exhibited significant plastic deformation before fracture.

Micro-compression Summary

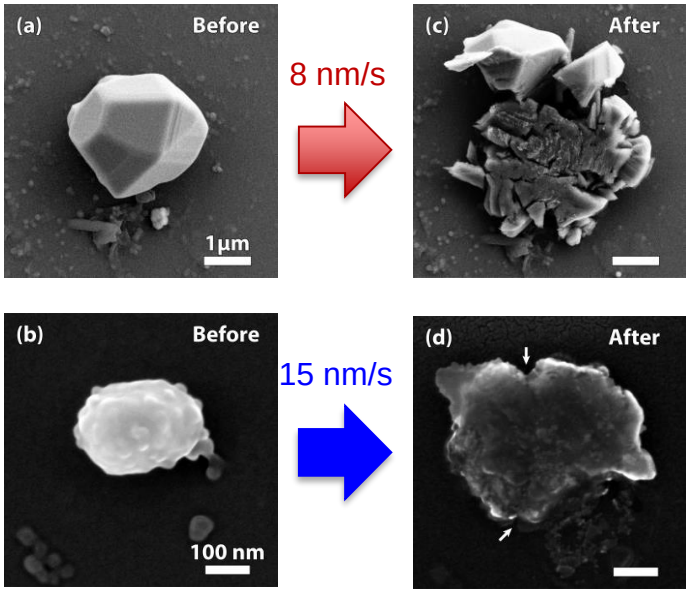

Particle Identifier	Diameter (µm)	Nominal Strain Rate (s^{-1})	Strain Energy Density Before Displacement Excursion (MJ/m^3)	Strain at displacement excursion (%)
Large Particles				
SEM-LP1	2.9	0.03	47	5
SEM-LP2	2.6	0.006	106	5
SEM-LP4	2.9	0.005	70	5
SEM-LP5	2.9	0.003	203	7
Avg Large Particles	**2.8**	-	**106±69**	**5.5 ± 1**
Small Particles				
SEM-SP2	0.17	0.09	494	11
SEM-SP3	0.29	0.05	366	12
SEM-SP4	0.28	0.05	607	13
SEM-SP5	0.29	0.05	675	16
*TEM-SA2	0.38	*0.005	573	32
*TEM-SB1	0.24	*0.009	1066	27
Avg Small Particles	**0.26**	-	**630±238**	**18 ± 9**

	Micron	Sub-micron
# Pre-existing Defects	High	Moderate
Energy Density Input	Low	Moderate
Governing Mechanism(s)	Fracture	Plasticity + Fracture
Response to Compression	Crack initiation & Propagation	Dislocation nucleation, slip, crack initiation & propagation

- Micron sized particles - brittle fracture
- Sub-micron sized particles - substantial plastic deformation before fracture and/or coordinated shear deformation.
  - **6x** higher strain energy density input
    - dislocation nucleation
  - **3x** higher accumulated strain
  - In some cases, became polycrystalline.

Ceramic Particle RT Deformation - Alumina

- Deformation behavior influenced by numbers of internal defects, orientation, size.

Verified

	Micron	Sub-micron	Single Crystal Nano	Bicrystal Nano
# Pre-existing Defects	High	Moderate	None	Grain Boundary
Energy Density Input	Low	Moderate	High	Low
Governing Mechanism(s)	Fracture	Plasticity + Fracture	Plasticity	Fracture
Response to Compression	Crack initiation & Propagation	Dislocation nucleation, slip, crack initiation & propagation	Dislocation nucleation, Slip	Crack initiation & propagation
Compression Testing	SEM	SEM and TEM	MD Simulation	MD Simulation

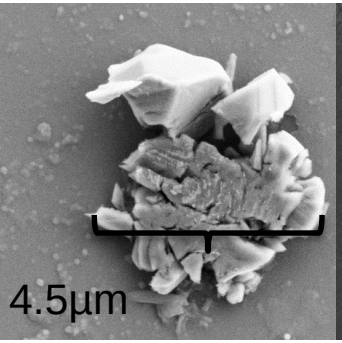

3.0µm - Fracture and Fragmentation

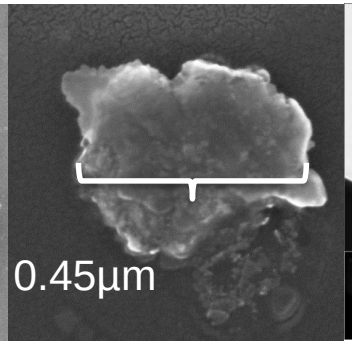

0.3µm – plastic deformation, shape change, cracking

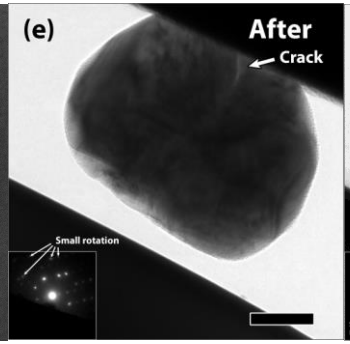

0.3µm - Dislocation Plasticity & through particle fracture

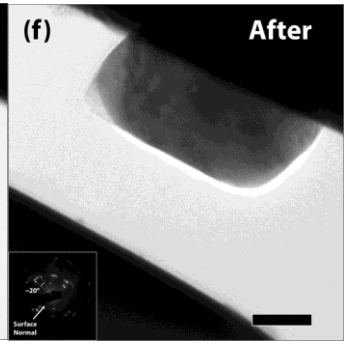

0.3µm - Coordinated Shear Deformation - Polycrystalline

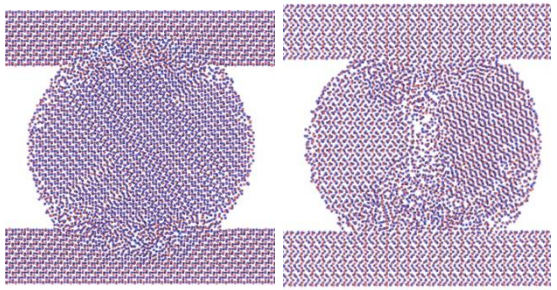

10 nm - Coordinated Shear Deformation **10 nm - Fracture**

MD Simulation Results

10 nm diameter, contain a GB, 'Janus' α-alumina,
20 m/s, left side randomly oriented and right side compression axis ⊥ (0001) → Fracture

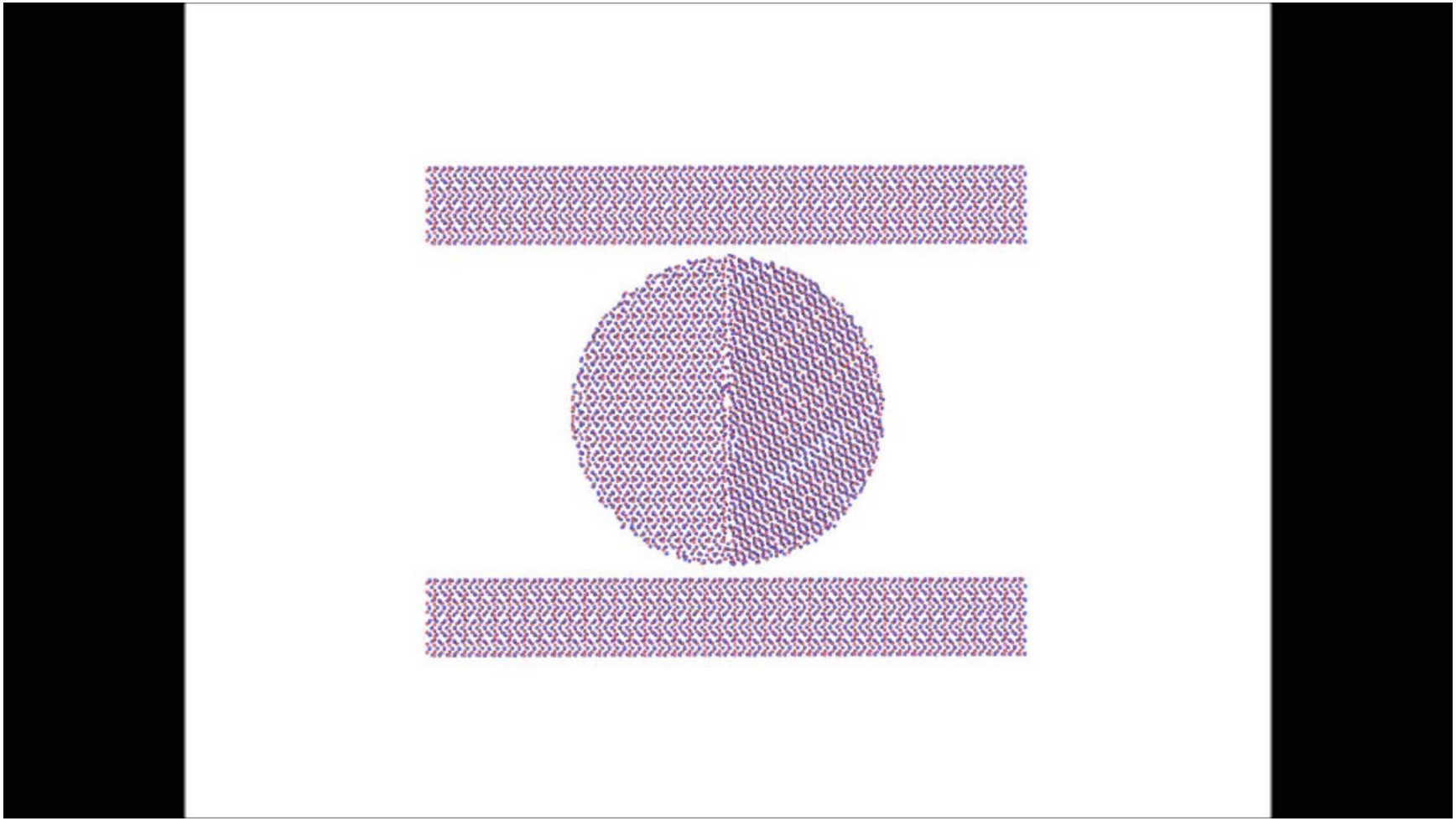

In Situ TEM Compression – P2

Zone axis near $[\bar{2}\ 5\ \bar{3}\ 2]$

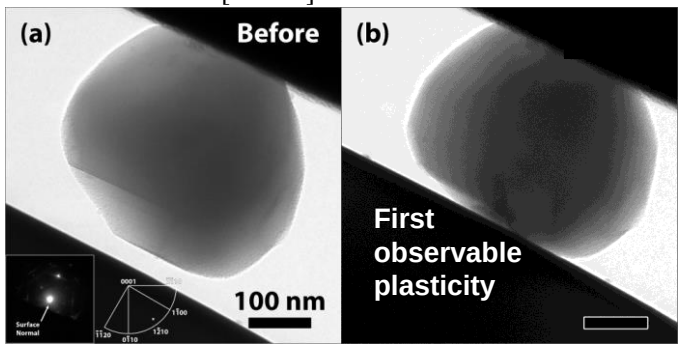

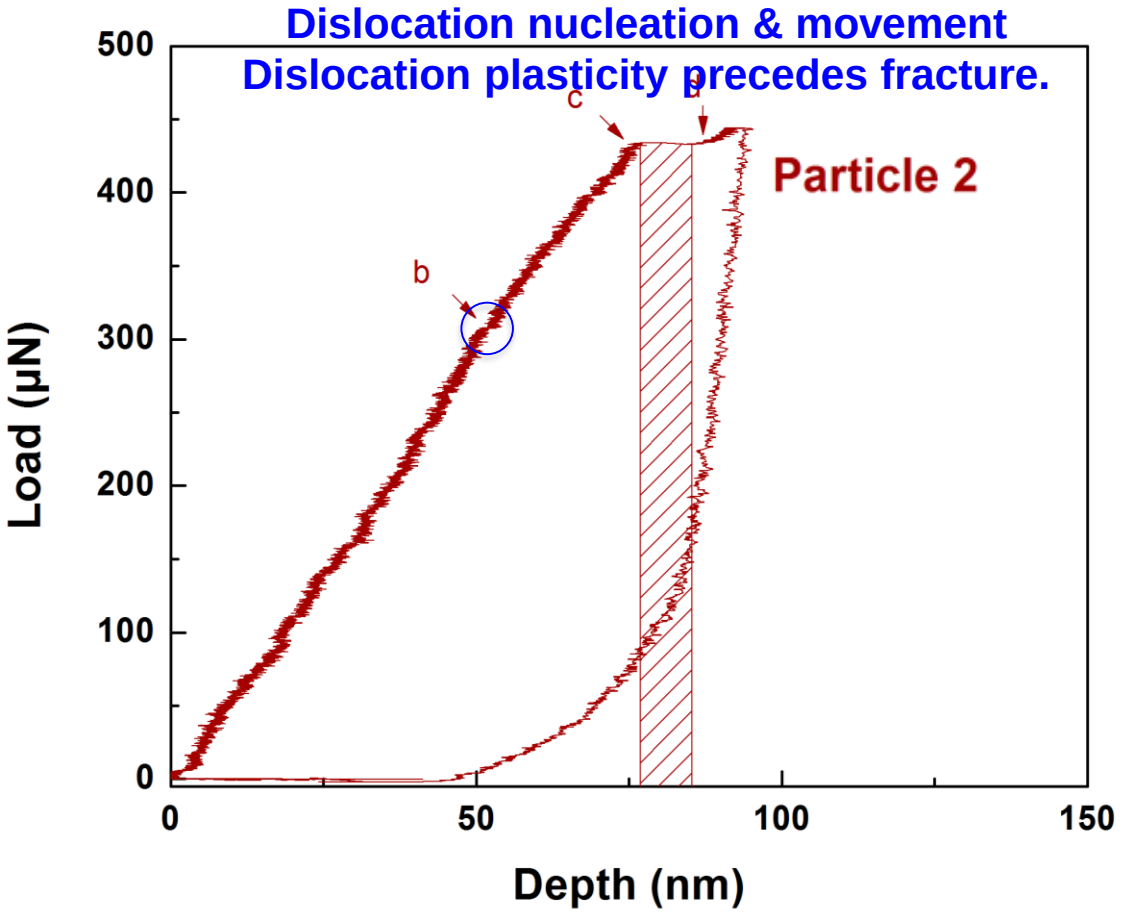

- Pre-burst plasticity: large regime with **high dislocation activity** (nucleation and moving through particle).

In Situ TEM Compression – P2

Zone axis near $[\bar{2}\ 5\ \bar{3}\ 2]$

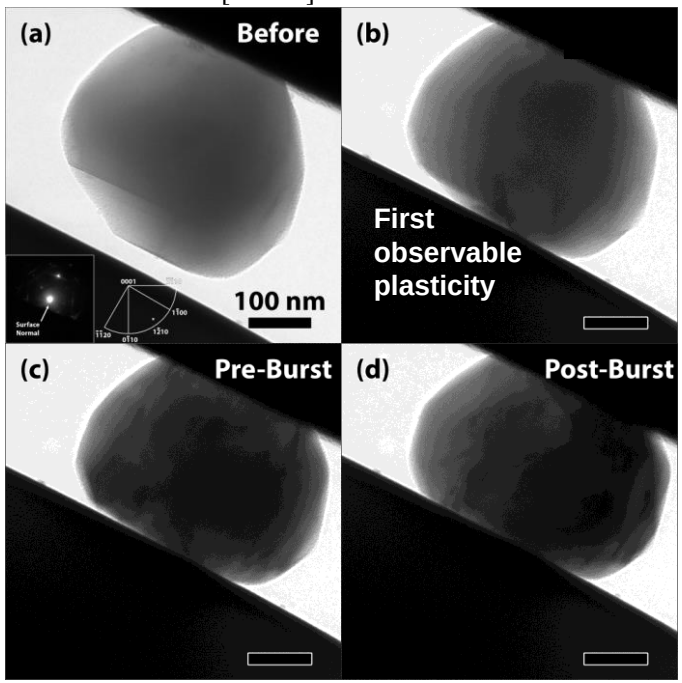

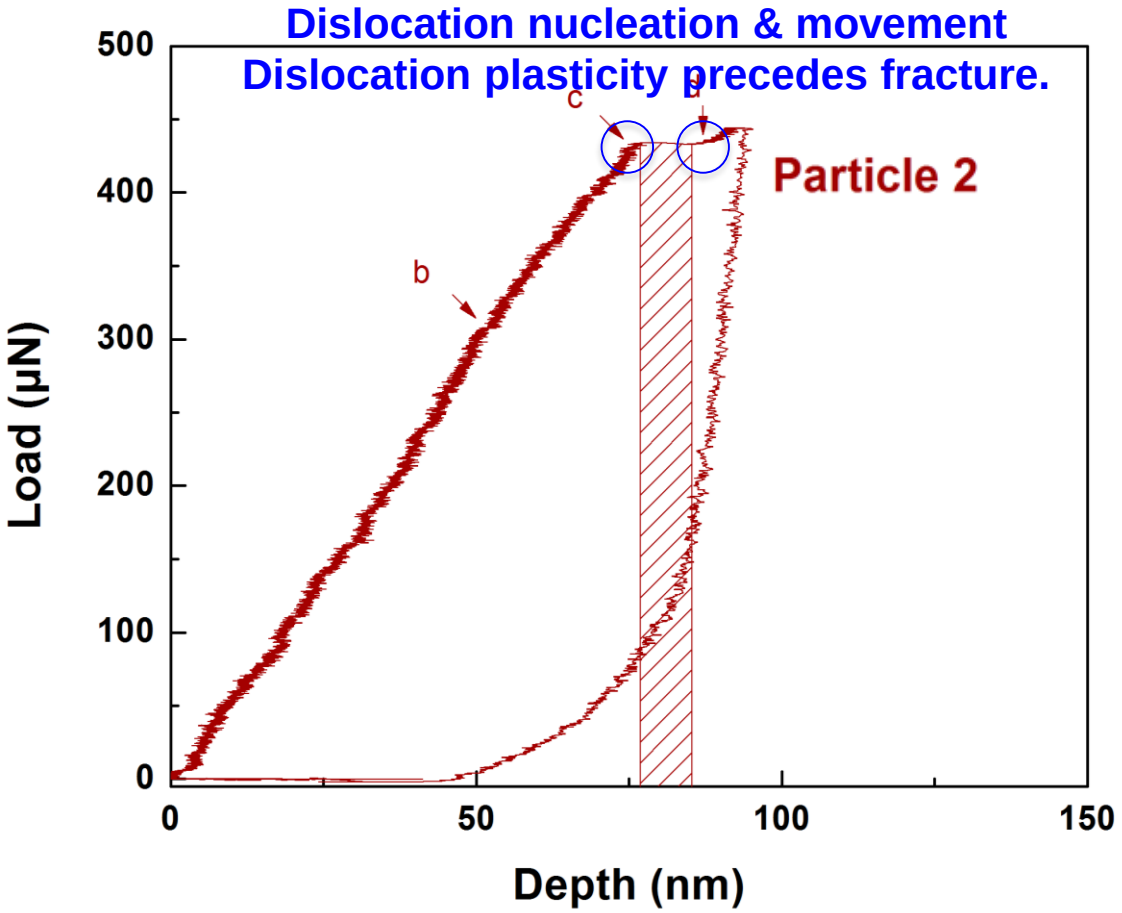

- Pre-burst plasticity: large regime with **high dislocation activity** (nucleation and moving through particle).
- **Crack nucleation and propagation** leading to through-particle fracture.

In Situ TEM Compression – P2

Zone axis near $[\bar{2}\ 5\ \bar{3}\ 2]$

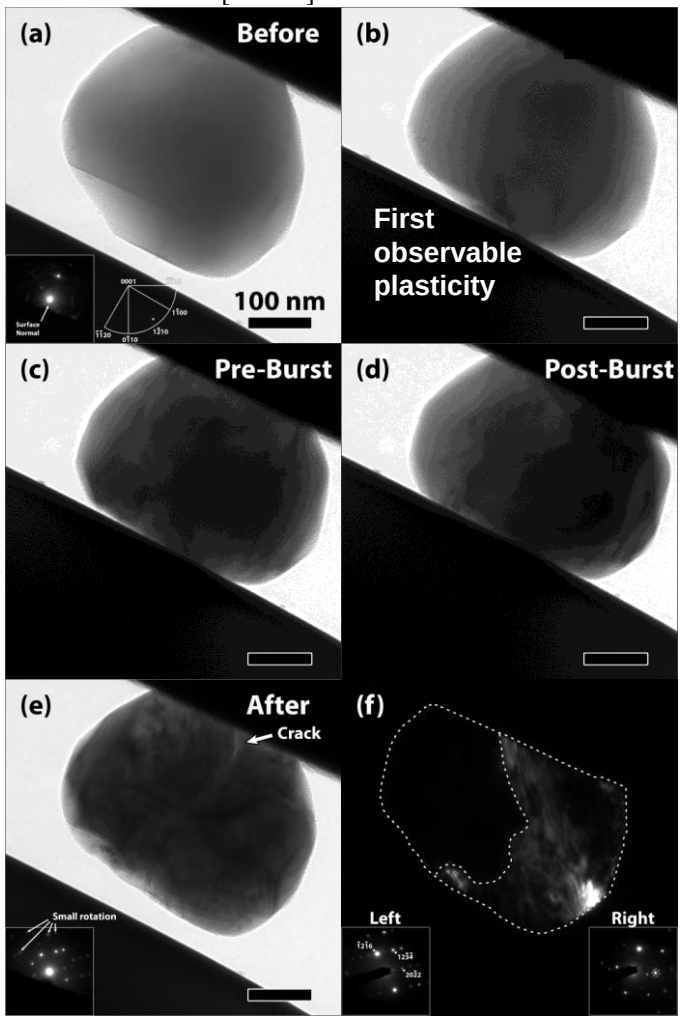

Two halves related by slight rotation, both near $[\bar{1}\ 2\ 1\ 6]$ zone axis

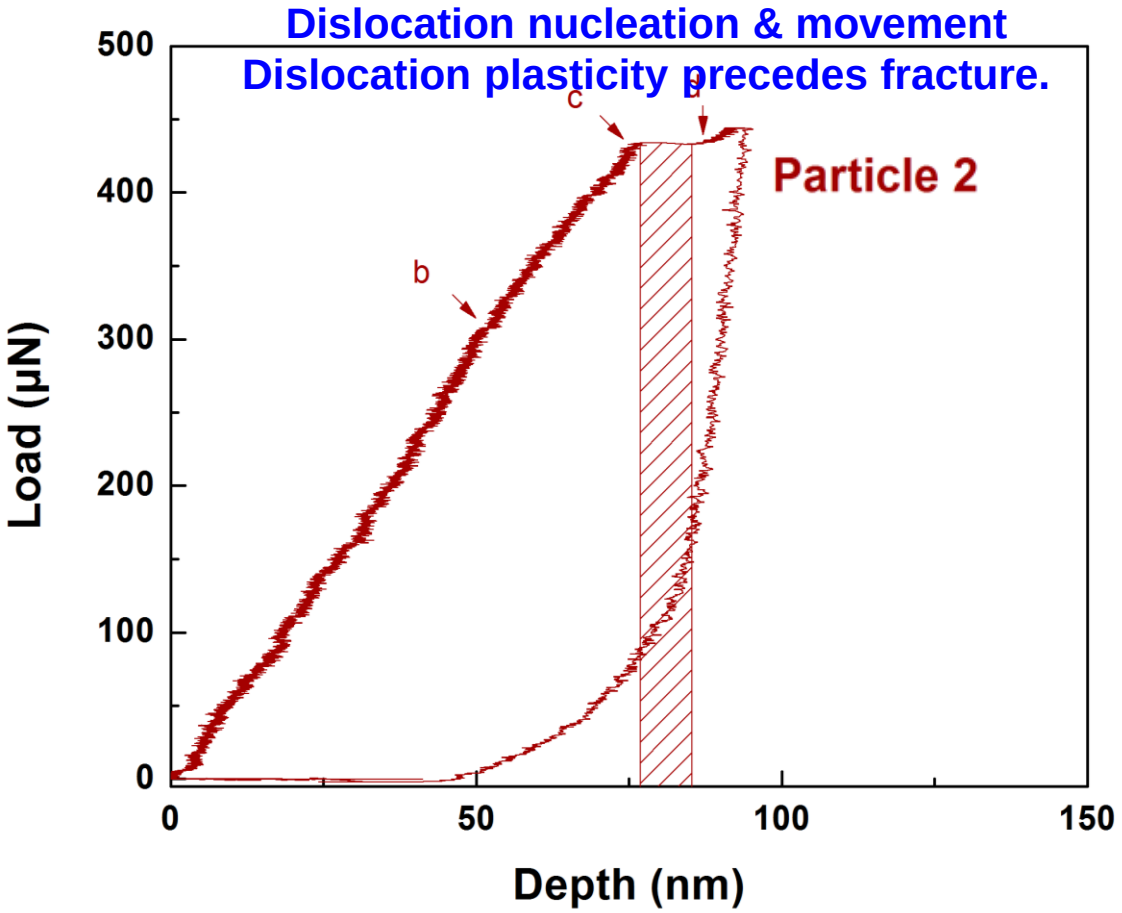

- Pre-burst plasticity: large regime with **high dislocation activity** (nucleation and moving through particle).
- **Crack nucleation and propagation** leading to through-particle fracture.

In Situ TEM Compression – P2

Diameter ~ 0.38 μm, Open loop, Strain rate ~0.005 s^{-1}

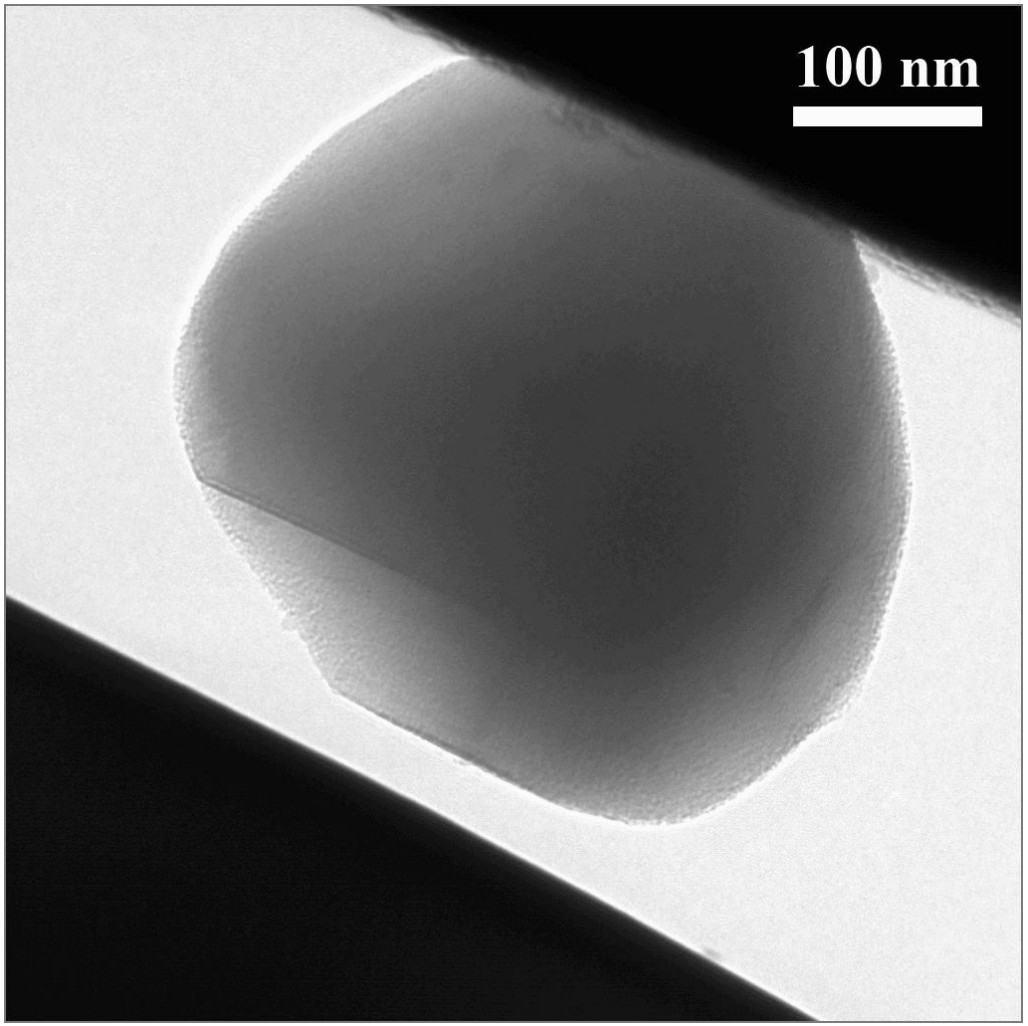

Dislocation nucleation & movement
Dislocation plasticity precedes fracture.

Large displacement gain at a constant load ("burst") corresponds to particle fracture.